# CHAPTER 4

# RESULTS AND DISCUSSION

## 4.1 Ternary System Based on Benzoxazine, Epoxy, and Phenolic Resins

The DSC thermograms in the temperature range of 30-300 °C at the heating rate of 10 °C/min of neat benzoxazine, epoxy, and phenolic novolac resins are shown in figure 4.1. An exothermic peak derived from the curing reaction is observed in benzoxazine monomer with a peak maximum at 225 °C. In the case of epoxy, the endothermic peak has been observed. It is maybe due to the evaporation of the monomer. However, for phenolic novolac, no sign of thermal event was observed.

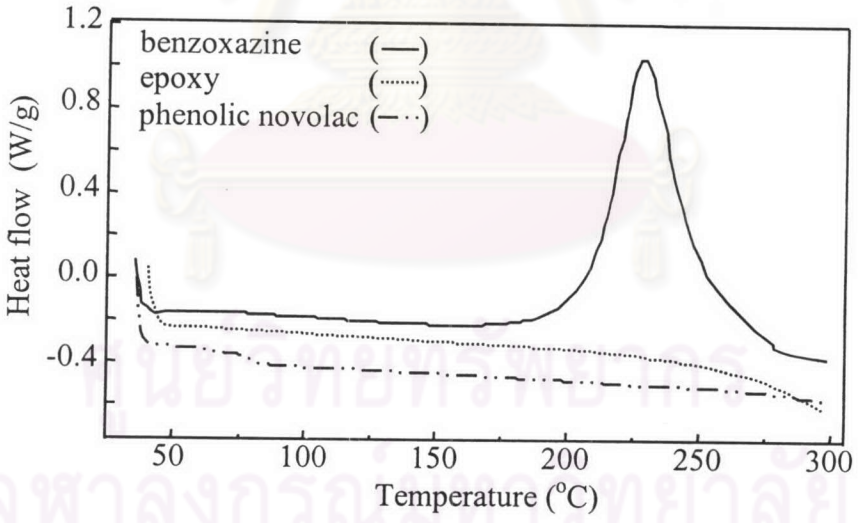


**Figure 4.1** DSC thermograms of raw material employed in this study.

Recently, Rimdusit and Tanthapanichkoon[37] reported the triangular diagram showing the relationship among the compositions at the temperature with 5% weight loss and percent residue at 800 °C of these ternary systems, as shown in figures 4.2

and 4.3 respectively. Rimdusit and Ishida[27,28] reported the effect of ternary system composition on curing behaviors and thermal transition, $T_g$, of these resins.

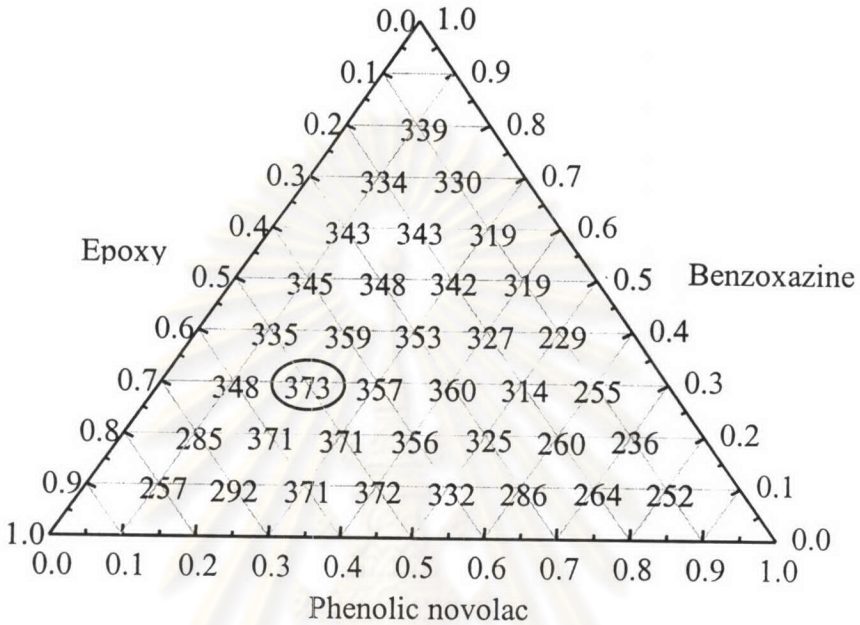


**Figure 4.2** Triangular diagram shows the temperature at 5% weight loss as a function of a composition of ternary systems.

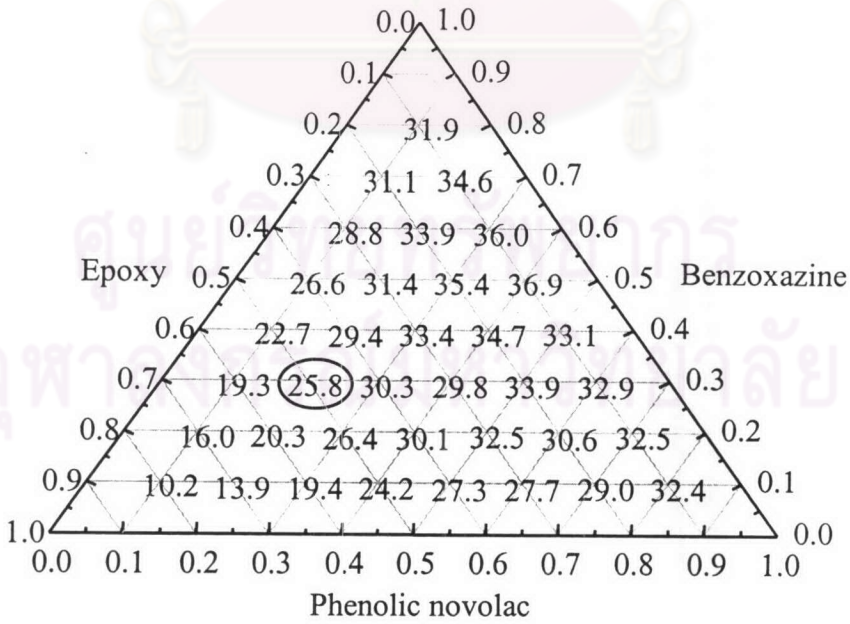


**Figure 4.3** Triangular diagram shows the percent residue at 800°C as a function of a composition of ternary systems.

One of the important properties of electronic packaging encapsulants is their thermal stability. As a result, the ternary mixture with the mass ratio of 3: 5: 2 of benzoxazine: epoxy: phenolic novolac resins has been chosen for investigation since it provides high thermal stability, optimal char yield suitable for the above application. The chosen ternary system presents maximum temperature at 5% weight loss in the triangular diagram. Figure 4.4 shows the DSC thermogram of BEP352. The curing peak position of BEP352 is about the same as that observed with polybenzoxazine homopolymer (i.e., about 240 °C). Figure 4.5 shows the FT-IR spectrum of BEP352 while the peak assignment of this resin is shown in table 4.1.

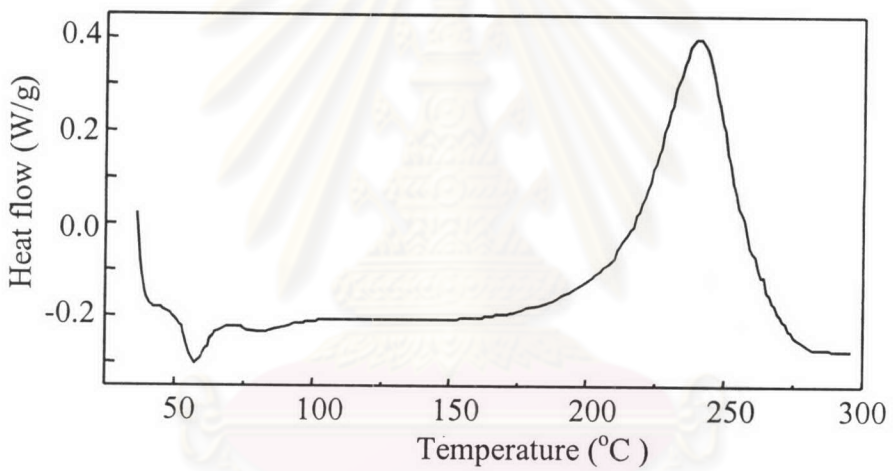


**Figure 4.4** DSC thermogram of BEP352.

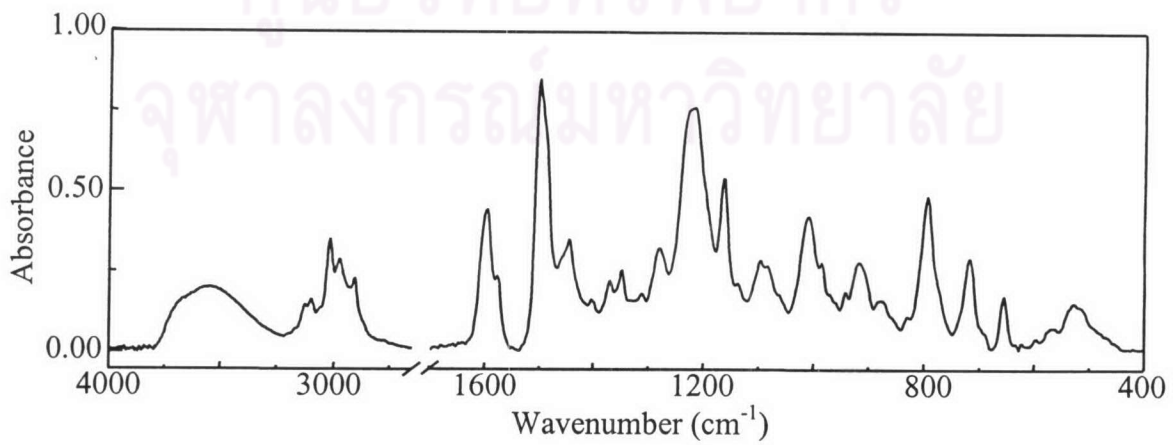


**Figure 4.5** FT-IR spectrum of BEP352.

**Table 4.1** Peak assignment of BEP352.

| Peak position ($cm^{-1}$) | Assignment |
|---|---|
| 3421 | O-H stretching of 2° alcohol |
| 3058 | C-H asymmetric stretching of methylene of epoxide ring |
| 3036 | C-H stretching of benzene ring |
| 2966 | C-H asymmetric stretching of methyl group |
| 2930 | C-H asymmetric stretching of methylene group |
| 2872 | C-H symmetric stretching of methyl group |
| 1602, 1508, 1456 | C=C stretching of benzene ring |
| 1383 | C-H symmetric deformation of geminated methyl group of bisphenol-A |
| 1296, 1235 | C-O(-Ar) asymmetric stretching of aliphatic aromatic ether |
| 1183 | C-H in plane deformation of 1,4-di-substitued of benzene ring |
| 1120 | C-H in plane deformation of 1,2,4-tri-substituted mode of oxazine ring |
| 1036 | C-O(-Ar) symmetric stretching of aliphatic aromatic ether |
| 946 | C-H out of plane deformation of 1,2,4-tri-substituted mode of oxazine ring |
| 913, 829 | C-O(-C) asymmetric stretching of epoxide ring |
| 755, 695 | C-H out of plane deformation of mono-substituted mode of benzene ring |

## 4.2 Curing Reaction of Monomer Systems

Figure 4.6 represents the temperature dependent FT-IR spectra of air due to high temperature in hot cell. The total energies detected by the detector increase as temperature increases. The shifts of baseline spectra have been observed. These phenomena have significant effect particularly in the low wavenumber region.

Not only the energy from the infrared light source reaches to detector but there are also some additional heats from hot cell. As a result, spectrum of air is affected by the increasing temperature.

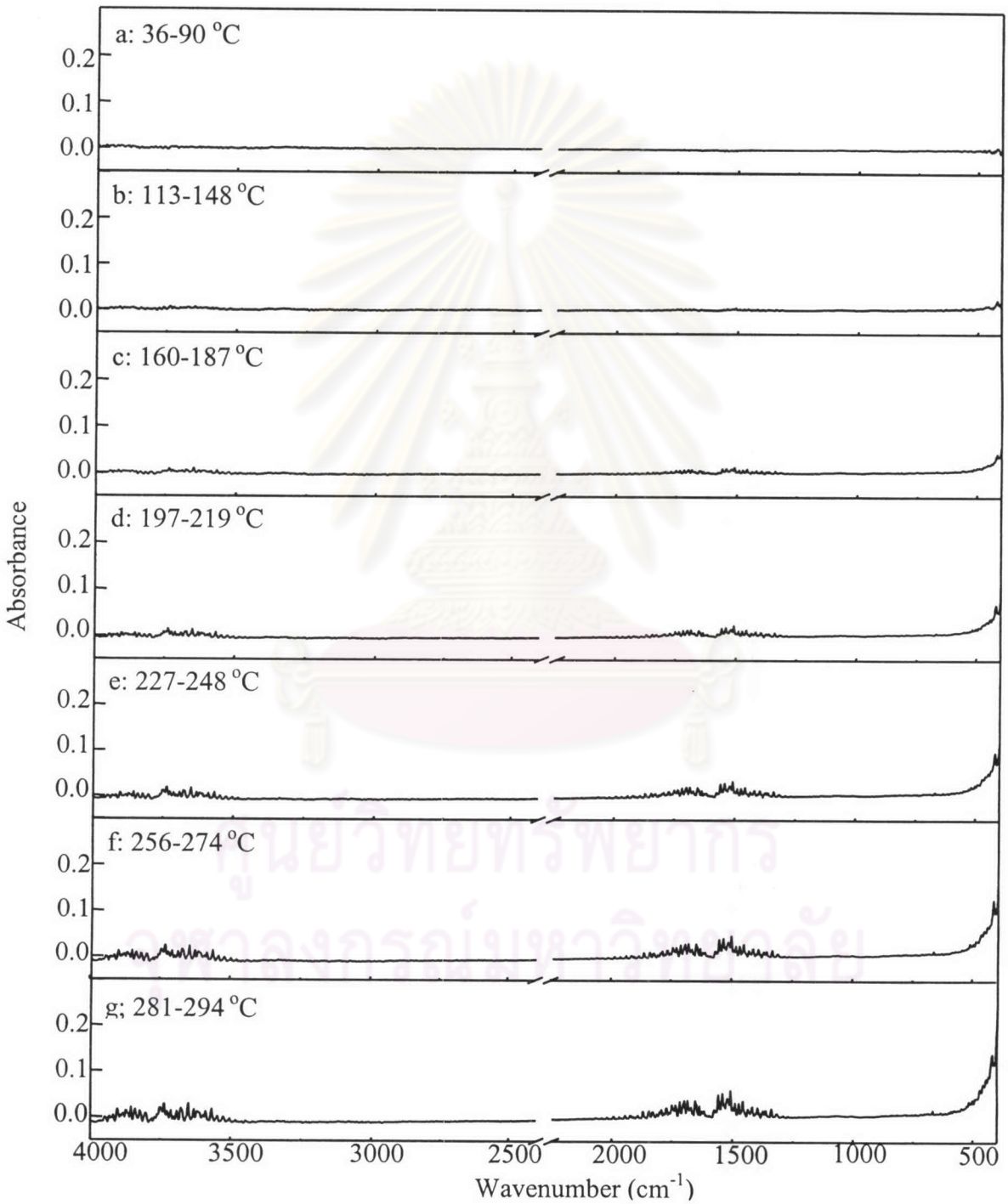


**Figure 4.6** The temperature dependent FT-IR spectra of air.

Figure 4.7 shows the FT-IR curing spectra of benzoxazine monomer at 100 °C. There is no change in the benzoxazine monomer because the benzoxazine ring is stable at 100 °C. Figure 4.8 shows the FT-IR curing spectra of benzoxazine monomer at 200 °C. However the ring-opening reaction of benzoxazine occurs at high temperature. As the curing process proceeds, large molecules are formed. There is the formation of an infinite three-dimension network. Some very highly branched and crosslinked molecules are formed. According to the polymerization mechanism reported by Dunkers and Ishida[38], the oxazine ring is opened by breakage of a C-O bond of oxazine ring. Then benzoxazine molecule transforms from a ring structure to a linear chain structure (as shown in figure 2.4). During this process, the tri-substituted benzene ring backbone of benzoxazine ring becomes tetra-substituted benzene ring. It leads to the formation of a phenolic Mannich base polybenzoxazine structure, (as shown in figure 4.9). A significant decrease of absorbance at 946 $cm^{-1}$, assigned to the oxazine ring, indicates that the ring-opening reaction of benzoxazine occurred. This is also confirmed by the appearance of new bands at 3500-3300 $cm^{-1}$, assigned to the phenolic hydroxyl group of oxazine species. Figure 4.10 shows an extent of reaction as a function of curing time observed at 946 $cm^{-1}$. This band is selected for further investigation of the ring-opening reaction of benzoxazine monomer.

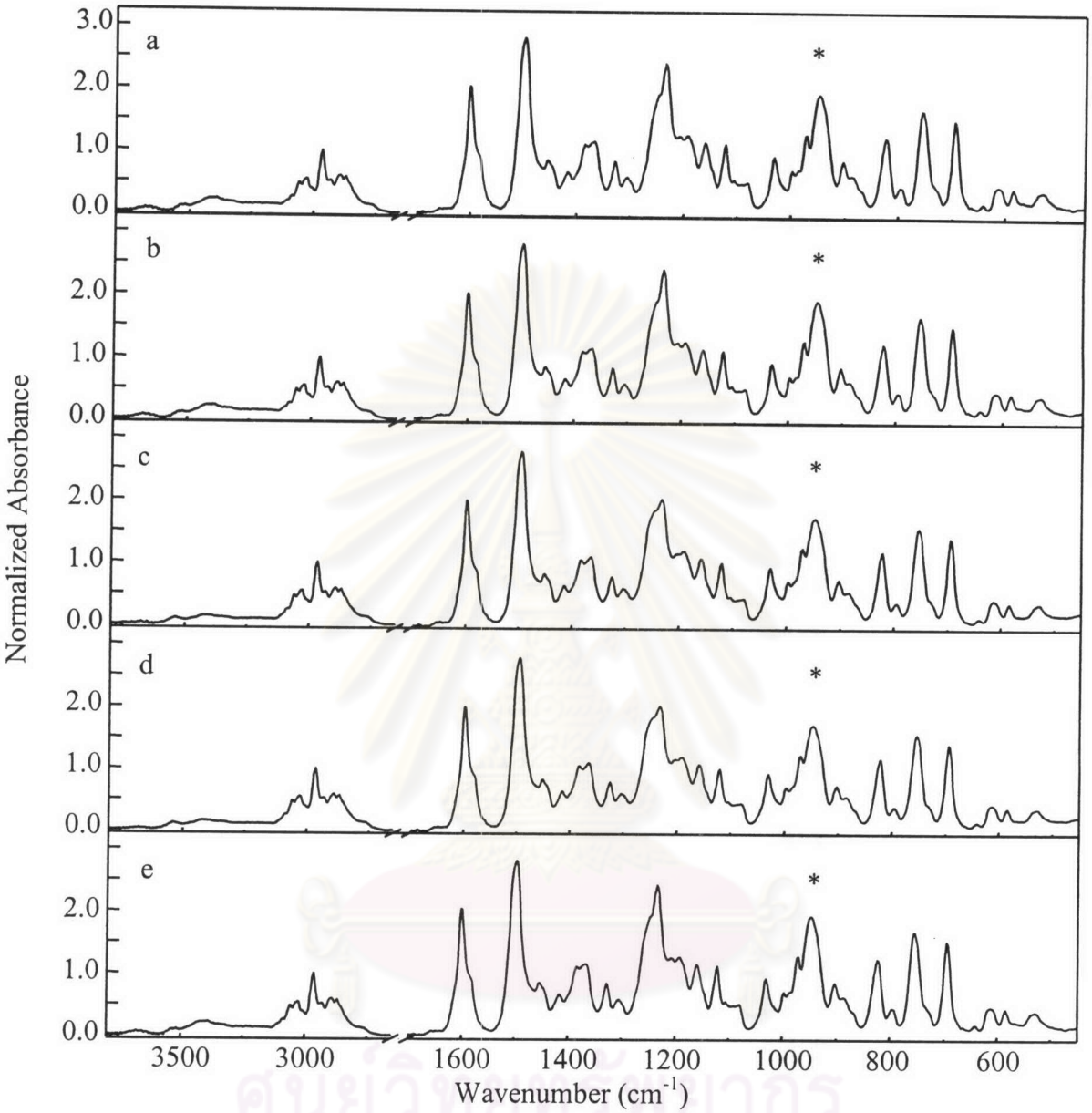


**Figure 4.7** FT-IR curing spectra of benzoxazine monomer. (a) before heating, (b) 100 °C, (c) 100 °C for 60 min, (d) 100 °C for 120 min, and (e) after cooling down to room temperature.

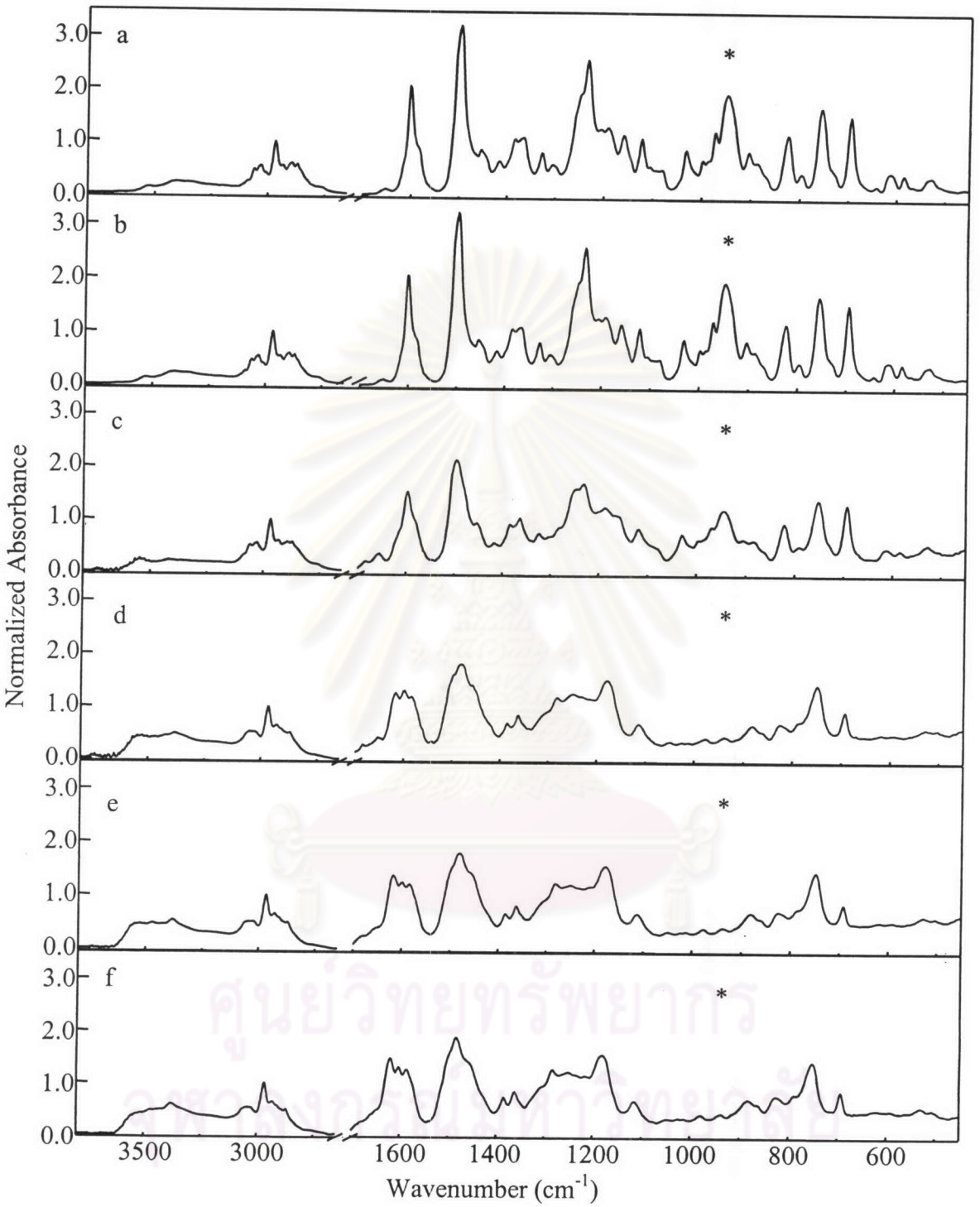


**Figure 4.8** FT-IR curing spectra of benzoxazine monomer. (a) before heating, (b) 200 °C, (c) 200°C for 10 min, (d) 200 °C for 60 min, (e) 200 °C for 120 min, and (f) after cooling down to room temperature.

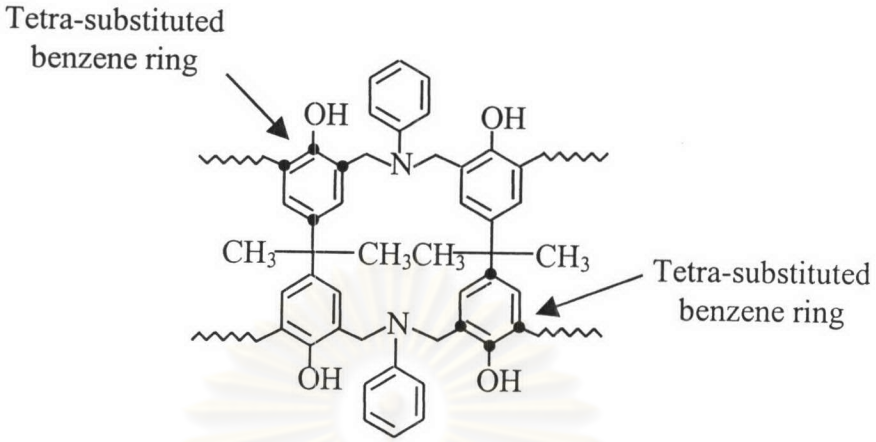


**Figure 4.9** The phenolic Mannich base network structure of benzoxazine monomer

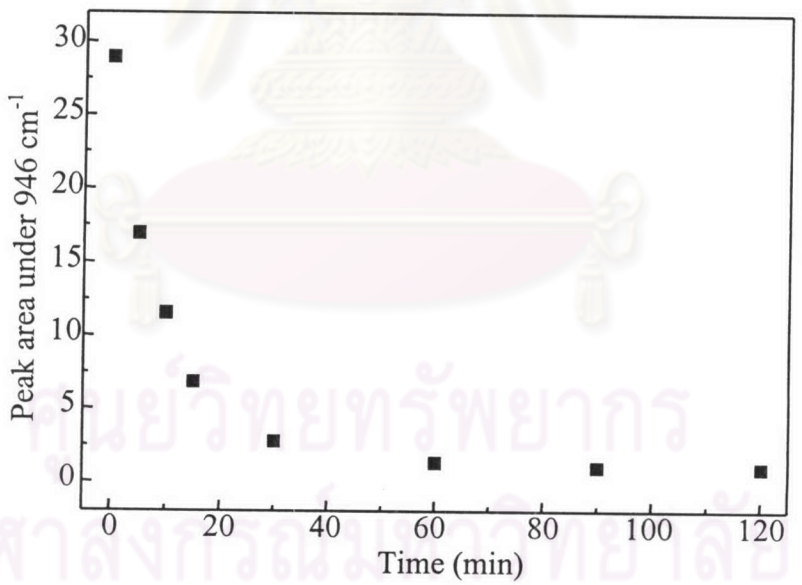


**Figure 4.10** Extent of the reaction observed at 946 $cm^{-1}$.

Figure 4.11 shows the FT-IR curing spectra of DGEBA epoxy resin at 100 °C. There is no spectral change. But at higher temperature, changes in the spectra are observed. Figure 4.12 shows the FT-IR curing spectra of DGEBA epoxy resin at 200 °C. These changes are due to the effect of heating inside the hot cell. When epoxy molecules received energy, changes in the vibration of chemical bonds are observed. But there is no any chemical reaction occurred because there is no any reactive species that can reacted with the epoxide ring in the system. In addition after heating, sample was cooled down to room temperature and spectrum again is taken again (figure 4.12 (e)). The spectrum exhibits a similar pattern as that of spectrum collect before heating (figure 4.12 (a)). It is a suitable index to confirm that there is no chemical change in the epoxy molecules up on heating to 200 °C. The small increase in absorption may be due to thickness change in the sample upon heating.

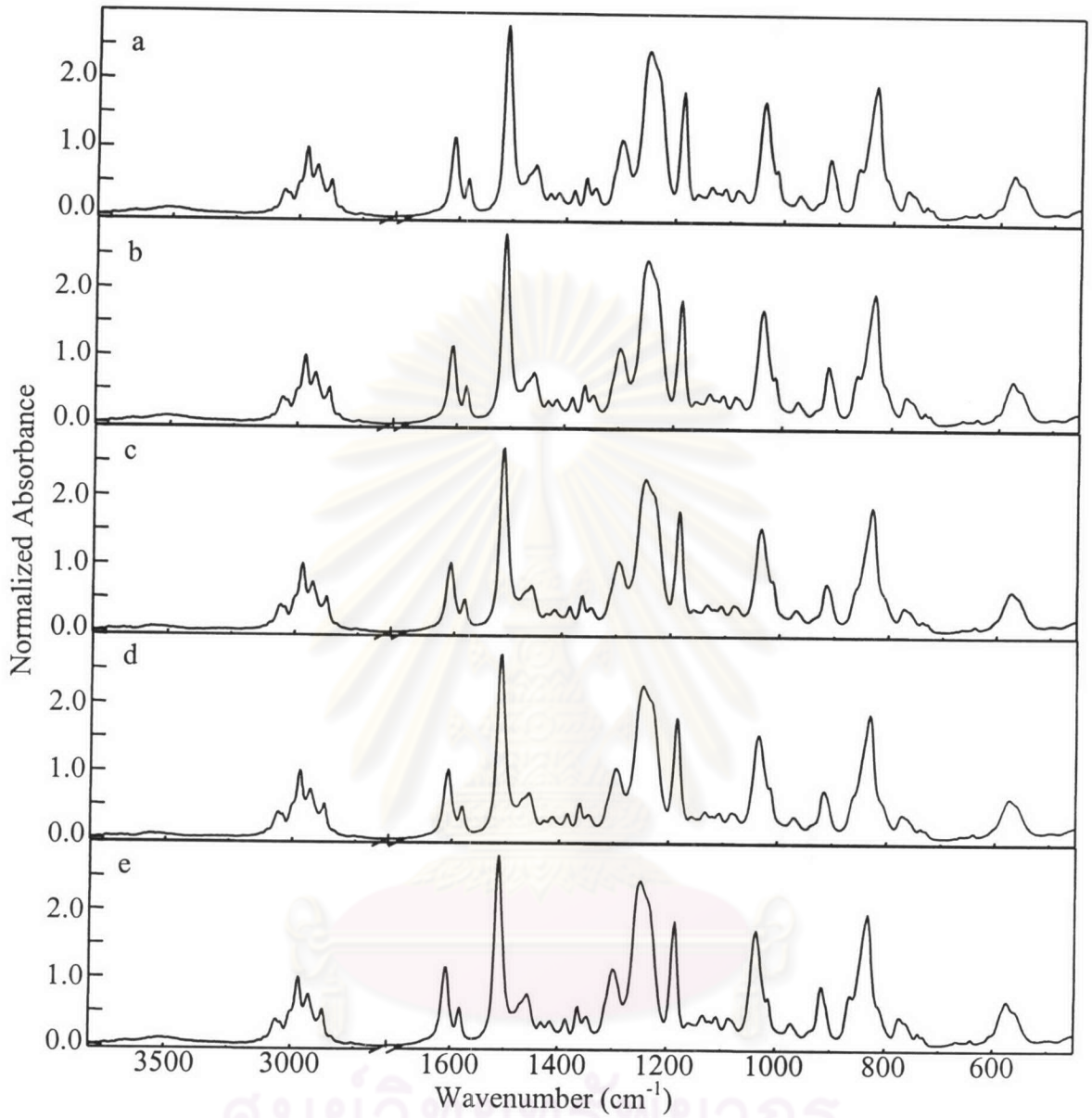


**Figure 4.11** FT-IR curing spectra of DGEBA epoxy resin. (a) before heating, (b) 100 °C, (c) 100 °C for 60 min, (d) 100 °C for 120 min, and (e) after cooling down to room temperature.

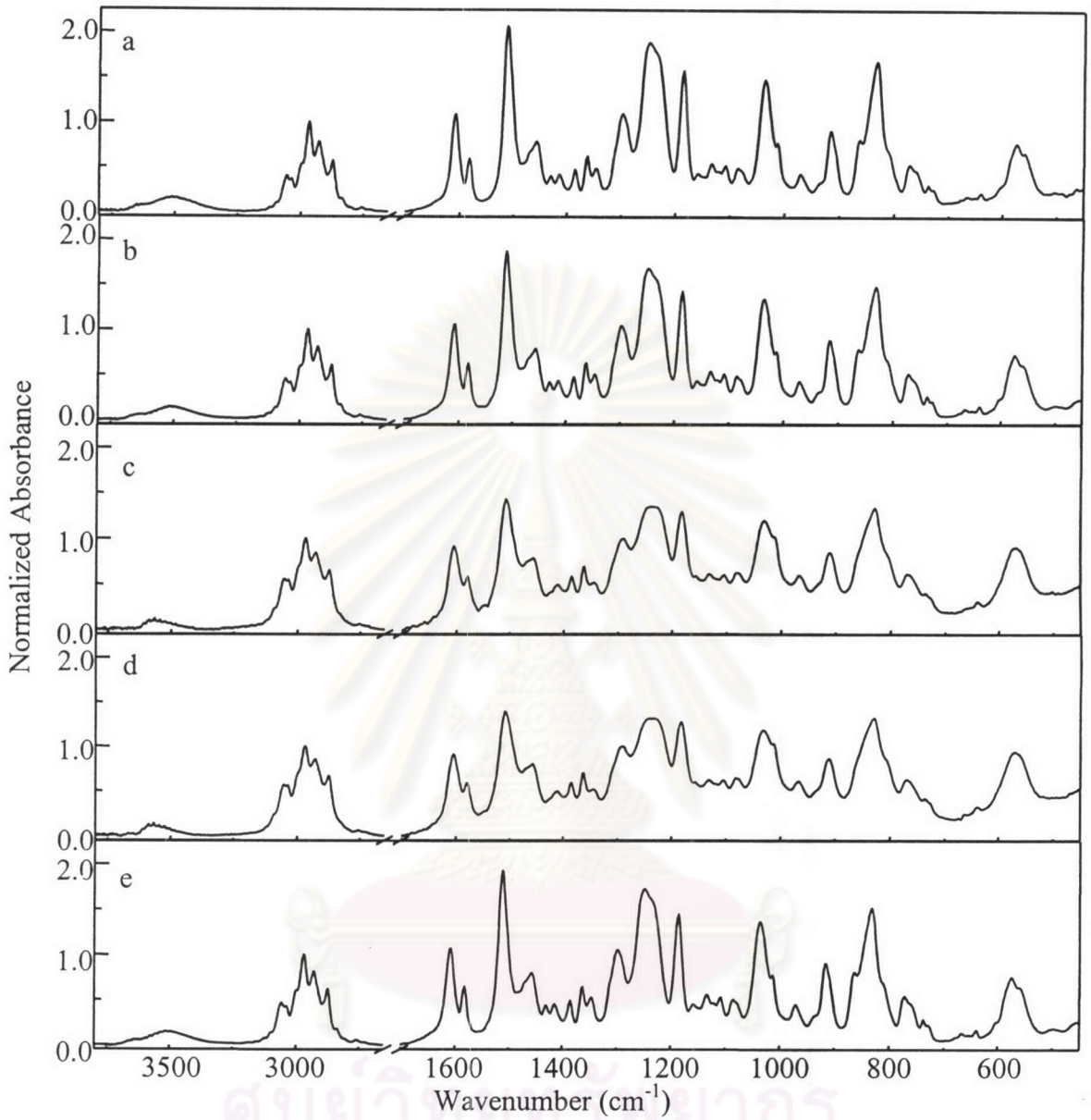


**Figure 4.12** FT-IR curing spectra of DGEBA epoxy resin. (a) before heating, (b) 200 °C, (c) 200 °C for 60 min, (d) 200 °C for 120 min, and (e) after cooling down to room temperature.

Figures 4.13 and 4.14 show FT-IR curing spectra of phenolic novolac resin at 100 °C and 200 °C, respectively. It has been reported that spectral changes in -OH stretching region (~3500 $cm^{-1}$) are due to the effect of hydrogen bonding, i.e., the intramolecular and intermolecular hydrogen bond.[26] Since the hydrogen bonds are sensitive to temperature, more free hydroxyl components are observed upon

increasing temperature. However there is no chemical change in the phenolic molecules.

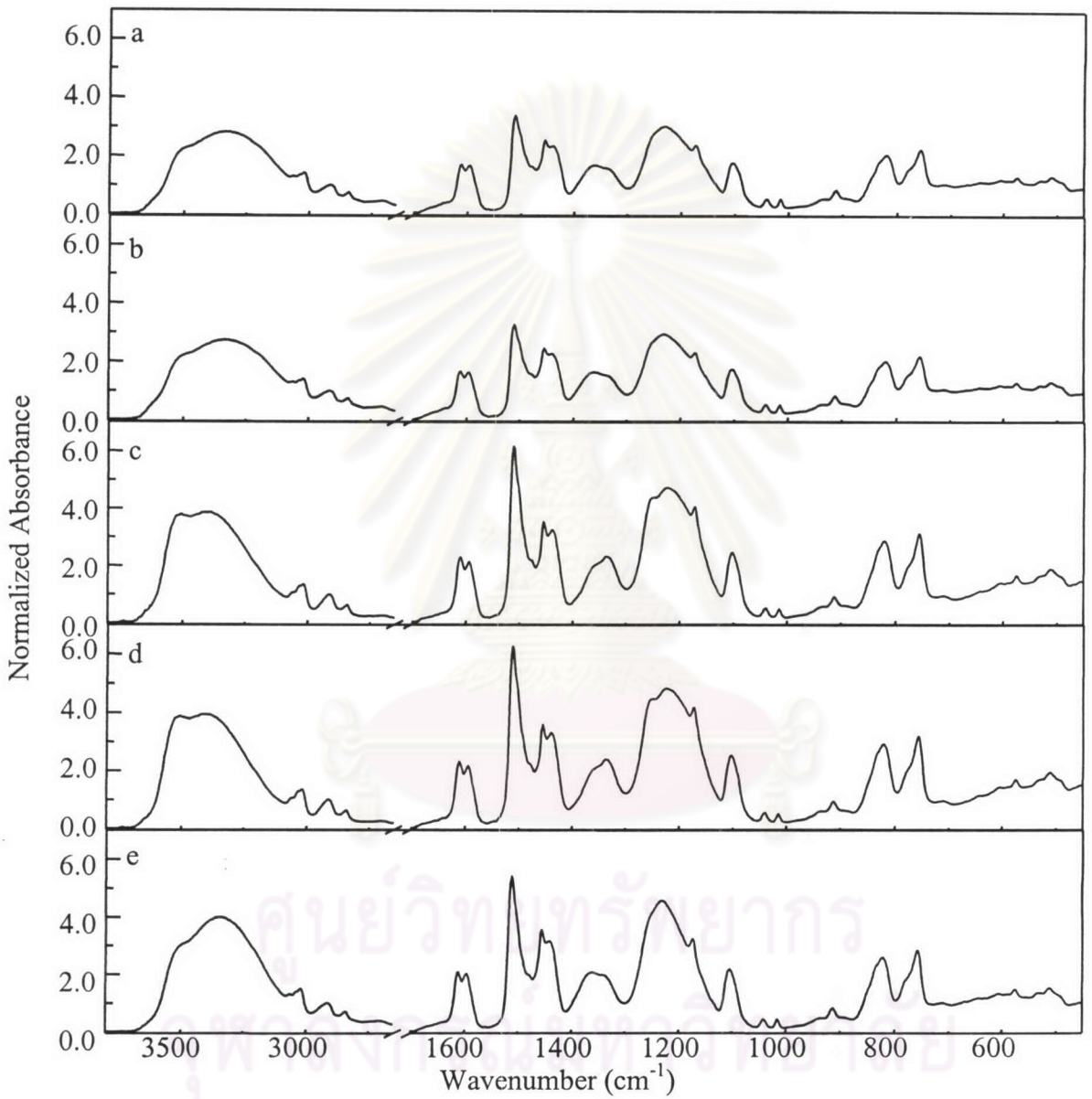


**Figure 4.13** FT-IR curing spectra of phenolic novolac resin. (a) before heating, (b) 100 °C, (c) 100 °C for 60 min, (d) 100 °C for 120 min, and (e) after cooling down to room temperature.

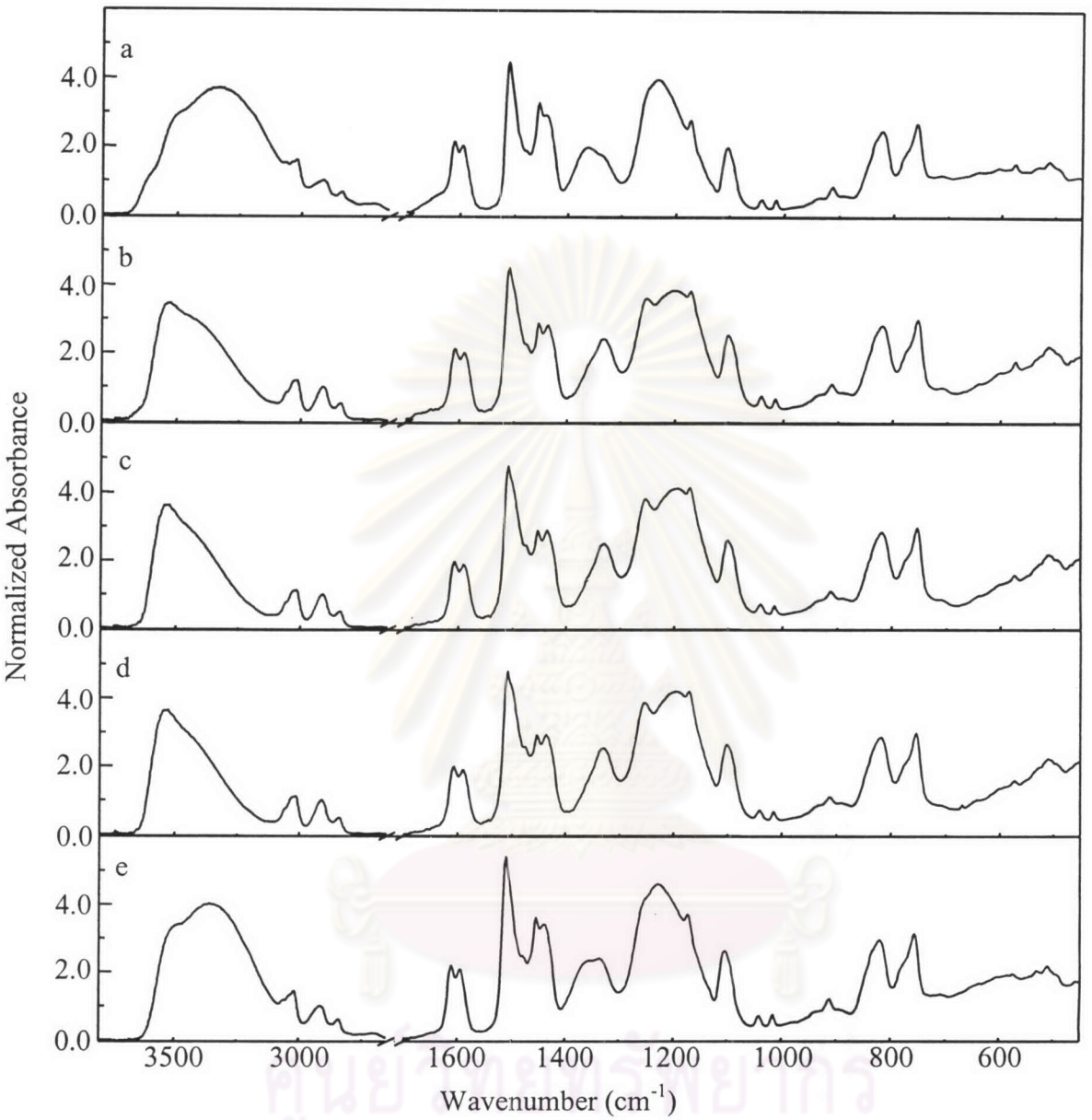


**Figure 4.14** FT-IR curing spectra of phenolic novolac resin. (a) before heating, (b) 200 °C, (c) 200 °C for 60 min, (d) 200 °C for120 min, and (e) after cooling down to room temperature.

## 4.3 Curing Reaction of Binary Systems

Figure 4.15 shows the DSC thermograms of the binary mixtures of benzoxazine and epoxy resins. At high benzoxazine fractions, there are shown only single peaks. At high epoxy fractions, the splitting of curing peaks are observed. Therefore, there are probably at least two chemical reactions occurred.[1] The first reaction is the polymerization reaction of benzoxazine, and the second is the copolymerization of benzoxazine and epoxy resins.

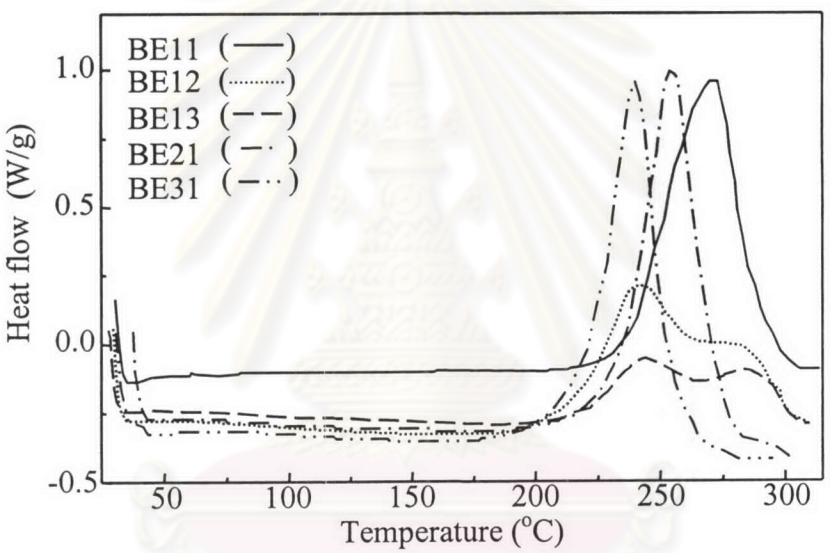


**Figure 4.15** DSC thermograms of the binary mixtures of benzoxazine and epoxy resins.

Figure 4.16 shows the FT-IR curing spectra of BE11 at 100 °C. There is no spectral change. This is because the ring-opening reaction of benzoxazine does not difficult to occur at 100 °C. Thus phenolic hydroxyl groups that contributed to the curing reaction are not under go chemical change upon heating. As a result, there are no any reactive species which can reacted with the epoxide ring. However at high temperature, the ring-opening reaction of benzoxazine occurs. So that not only the polymerization of benzoxazine monomer occurs but the copolymerization reaction of benzoxazine and epoxy occurs as well. Figures 4.17 and 4.18 show the FT-IR curing spectra of BE11 and BE12 at 200 °C, respectively. At the end of reaction, the

absorbance at 913 $cm^{-1}$, assigned to the epoxide ring, disappeared. But the absorbance at 946 $cm^{-1}$ still remains (figure 4.17 (e) and 4.18 (e)). In the polybenzoxazine homopolymer, this band has disappeared within 60 minutes (figure 4.8 (d)). It indicates that the copolymerization of benzoxazine and epoxy occurs faster than polybenzoxazine homopolymerization. After the ring-opening reaction of benzoxazine, the phenolic hydroxyl group generated by the ring-opening reaction can react with epoxide ring more easily than that with benzoxazine monomer. However at high benzoxazine fraction, this phenomenon is not observed. Figure 4.19 shows the FT-IR curing spectra of BE21 at 200 °C. At the end of reaction, the absorption intensity at 946 $cm^{-1}$ disappeared. Figure 4.20 shows an extent of reaction at 946 $cm^{-1}$ as a function of curing time of binary mixtures of benzoxazine and epoxy resins.

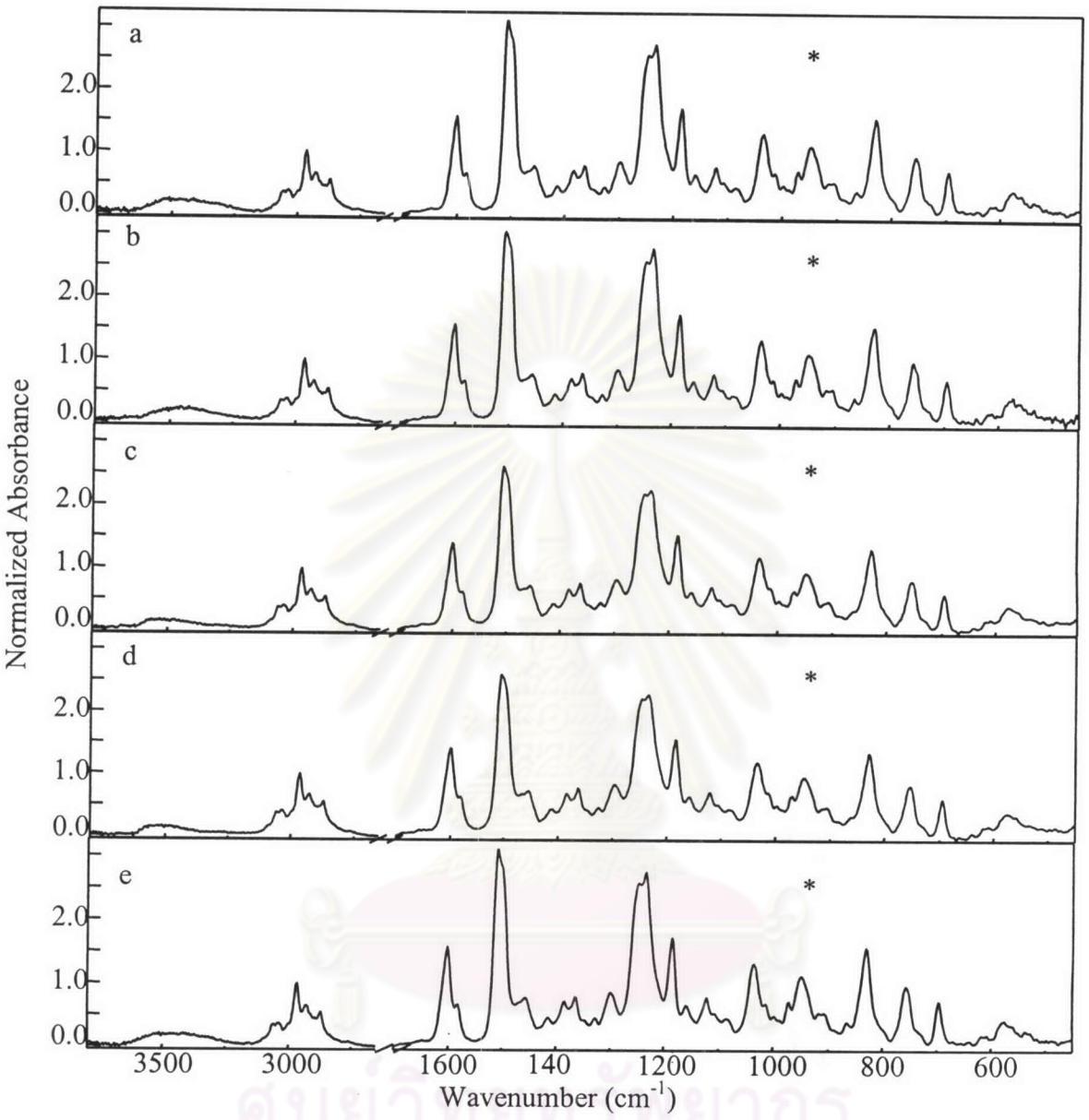


**Figure 4.16** FT-IR curing spectra of BE11. (a) before heating, (b) 100 °C, (c) 100 °C for 60 min, (d) 100 °C for 120 min, and (e) after cooling down to room temperature.

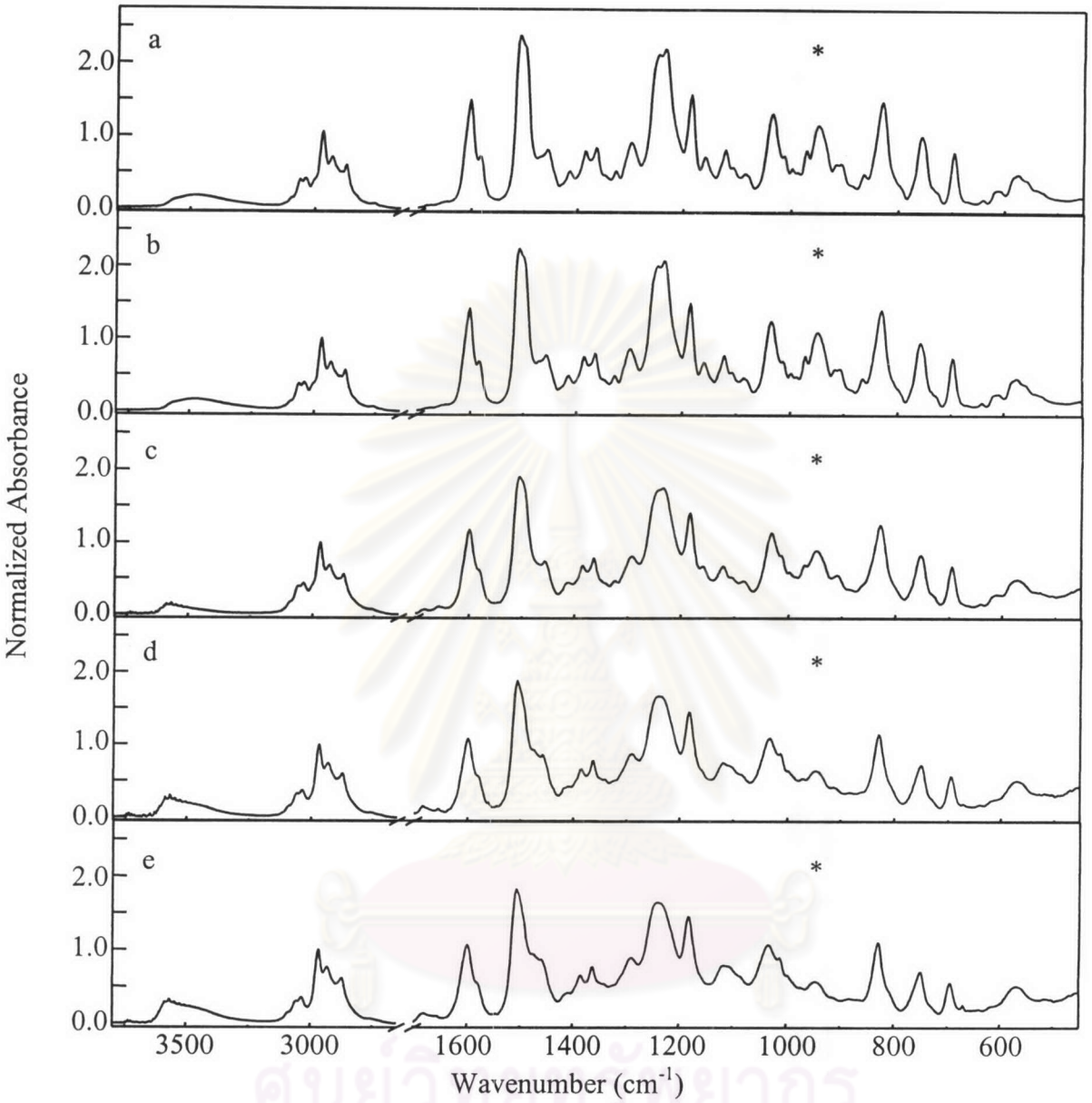


**Figure 4.17** FT-IR curing spectra of BE11. (a) before heating, (b) 200 °C, (c) 200 °C for 10 min, (d) 200 °C for 60 min, and (e) 200 °C for 120 min.

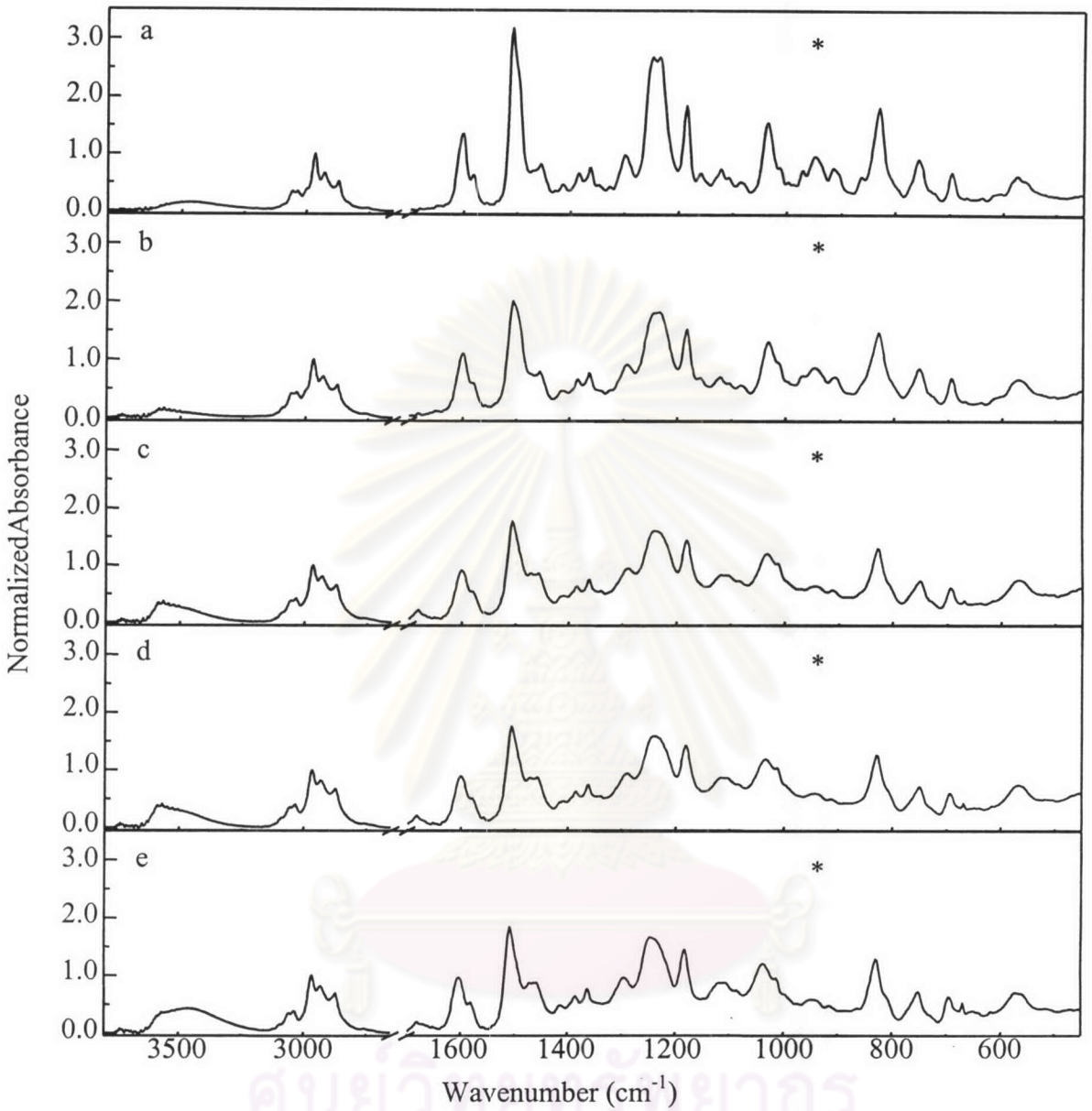


**Figure 4.18** FT-IR curing spectra of BE12. (a) before heating, (b) 200 °C, (c) 200 °C for 60 min, (d) 200 °C for 120 min, and (e) after cooling down to room temperature.

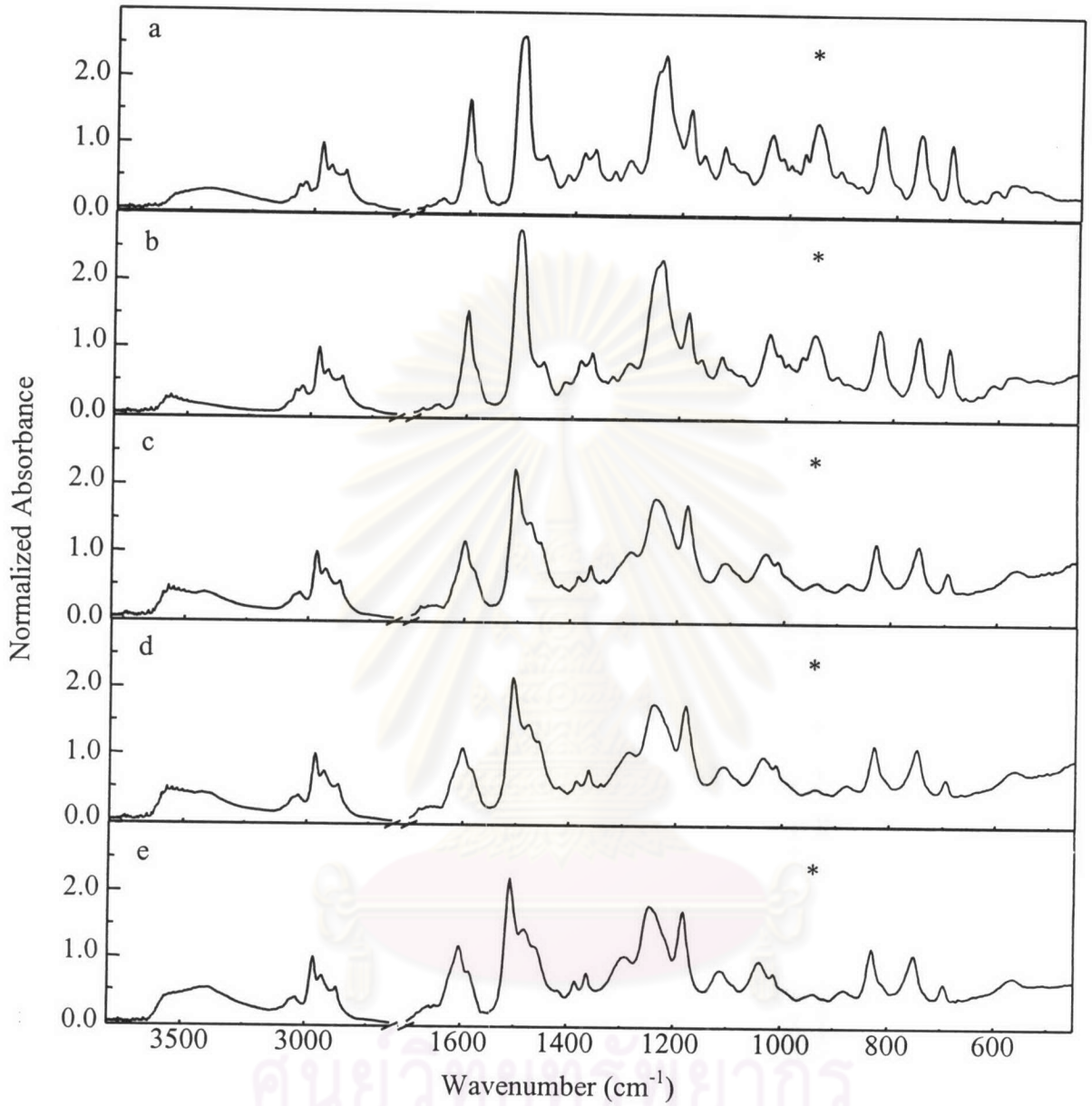


**Figure 4.19** FT-IR curing spectra of BE21. (a) before heating, (b) 200 °C, (c) 200 °C for 60 min, (d) 200 °C for 120 min, and (e) after cooling down to room temperature.

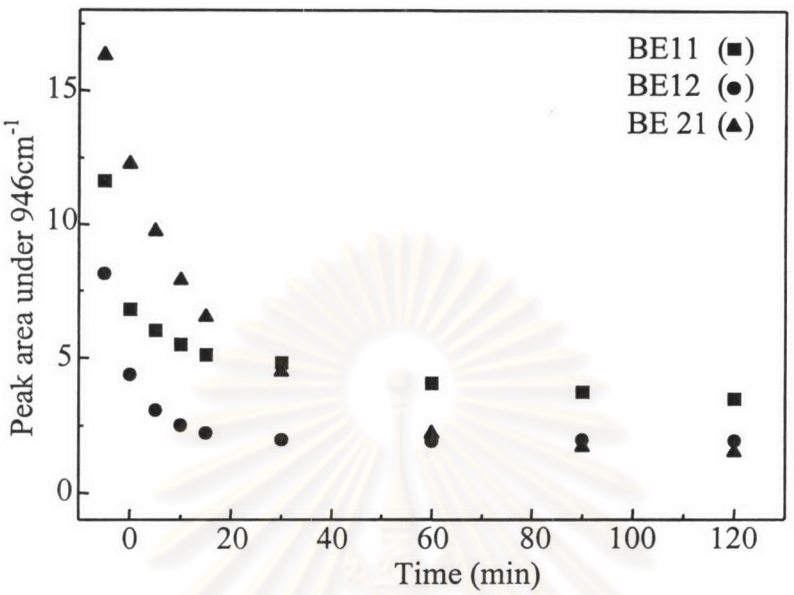


**Figure 4.20** Extent of the reaction observed at 946 $cm^{-1}$.

Figure 4.21 shows the DSC thermogram of the binary mixtures of benzoxazine and phenolic novolac resin. The binary systems exhibit lower curing peaks than that of polybenzoxazine homopolymer. Figure 4.22 represents the FT-IR curing spectra of BP11 at 100 °C. It shows the decrease of absorbance at 946 $cm^{-1}$ as a function of curing time. This is in good agreement with the previous reported[17] that the existence of phenolic novolac with free phenolic hydroxyl structure could accelerated the ring-opening reaction of benzoxazine. As a result, the ring-opening reaction of benzoxazine with phenolic novolac resin can be proceeded at a lower temperature than polybenzoxazine homopolymer. Figure 4.23 shows the FT-IR curing spectra of BP11 at 200 °C. The absorption intensity at 946 $cm^{-1}$ starts to decrease within 10 minutes. In contrast with the result in polybenzoxazine homopolymer (figure 4.8), this peak has disappeared within 30 minutes. Figures 4.24 and 4.25 show the FT-IR curing spectra of BP12 and BP21 at 200 °C, respectively. It demonstrates that the cure times of binary mixtures are reduced with the increasing of phenolic novolac resin. Figure 4.26 shows the extent of reaction at 946 $cm^{-1}$ as a function of curing time of binary mixtures of benzoxazine and phenolic novolac resins.

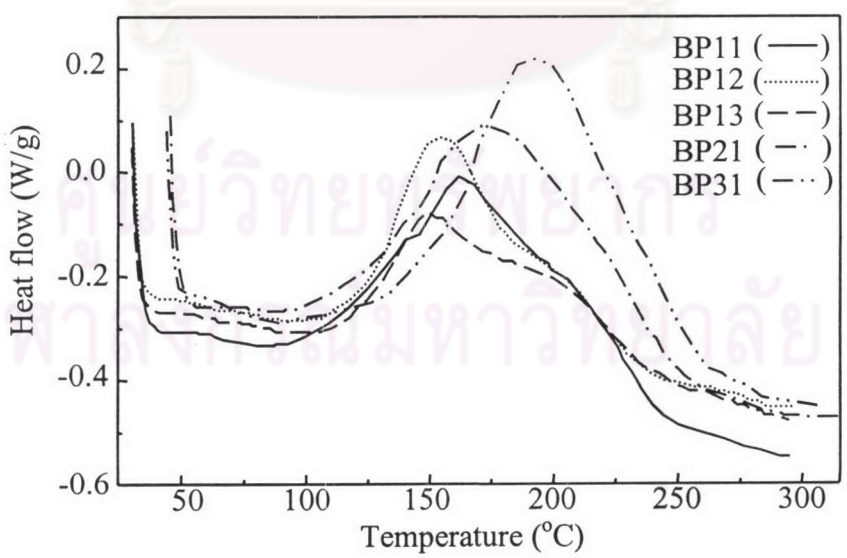


**Figure 4.21** DSC thermograms of the binary mixtures of benzoxazine and phenolic novolac resins.

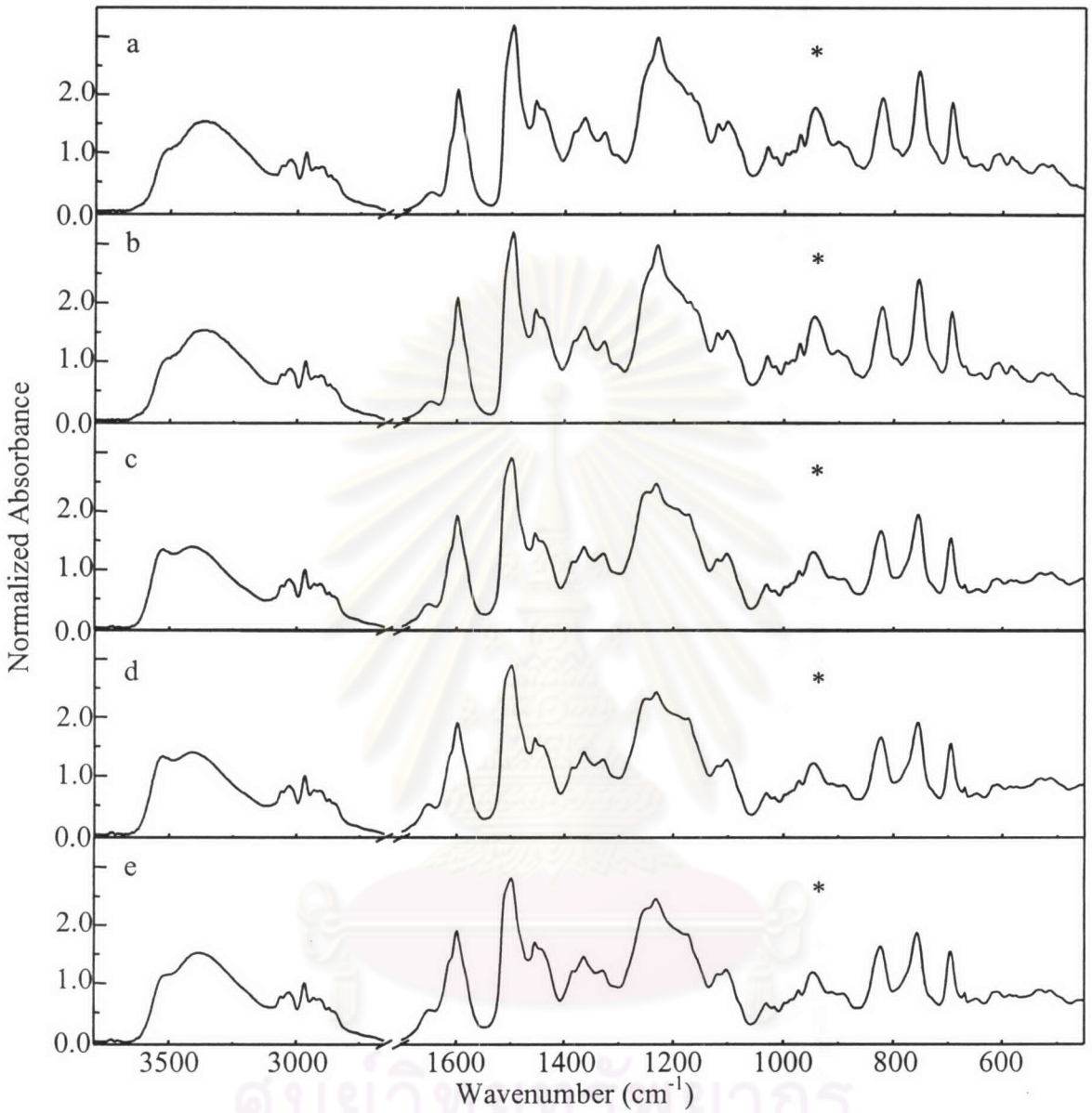


**Figure 4.22** FT-IR curing spectra of BP11. (a) before heating, (b) 100 °C, (c) 100 °C for 60 min, (d) 100 °C for 120 min, and (e) after cooling down to room temperature.

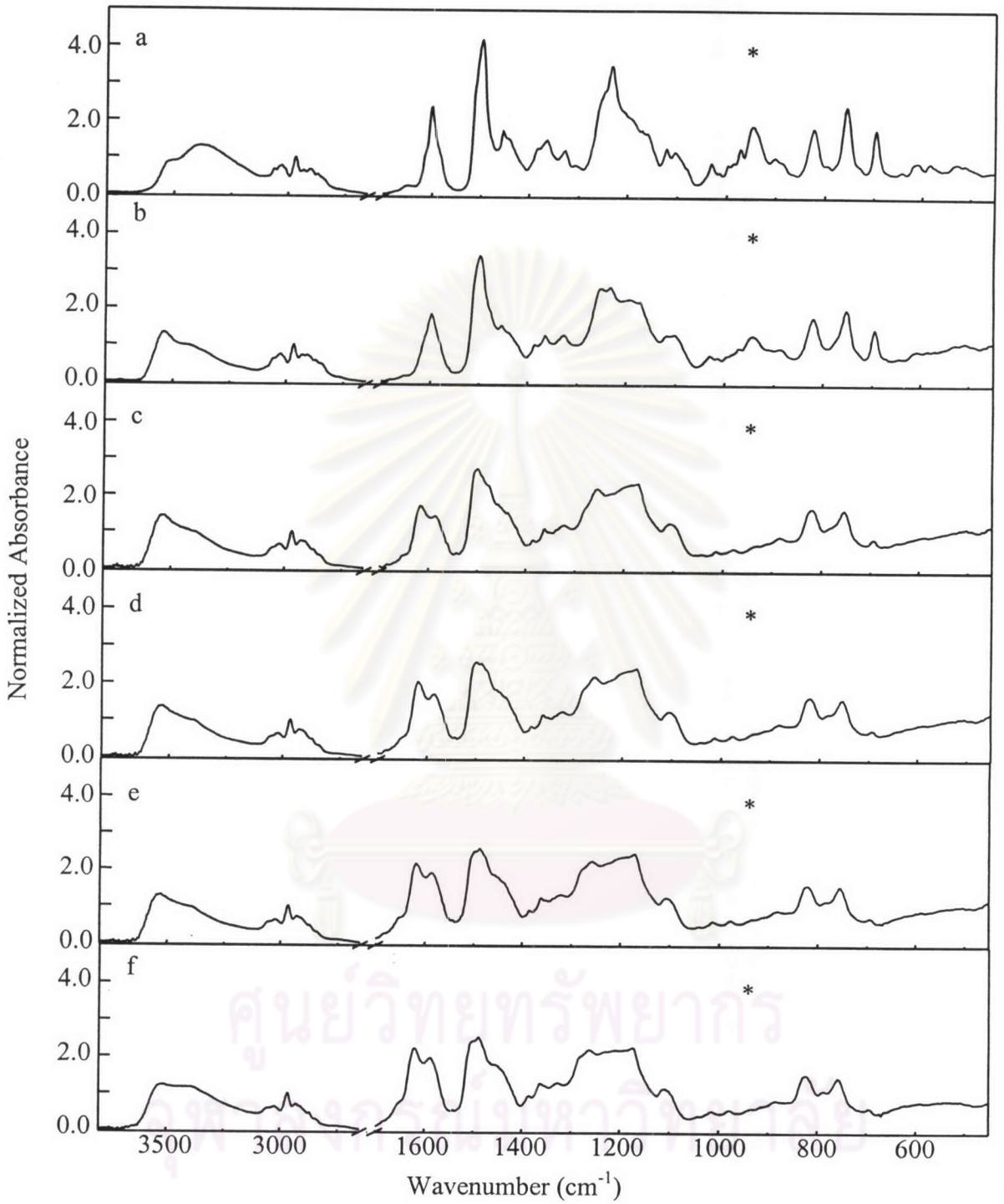


**Figure 4.23** FT-IR curing spectra of BP11. (a) before heating, (b) 200 °C, (c) 200 °C for 10 min, (d) 200 °C for 60 min, (e) 200 °C for 120 min, and (f) after cooling down to room temperature.

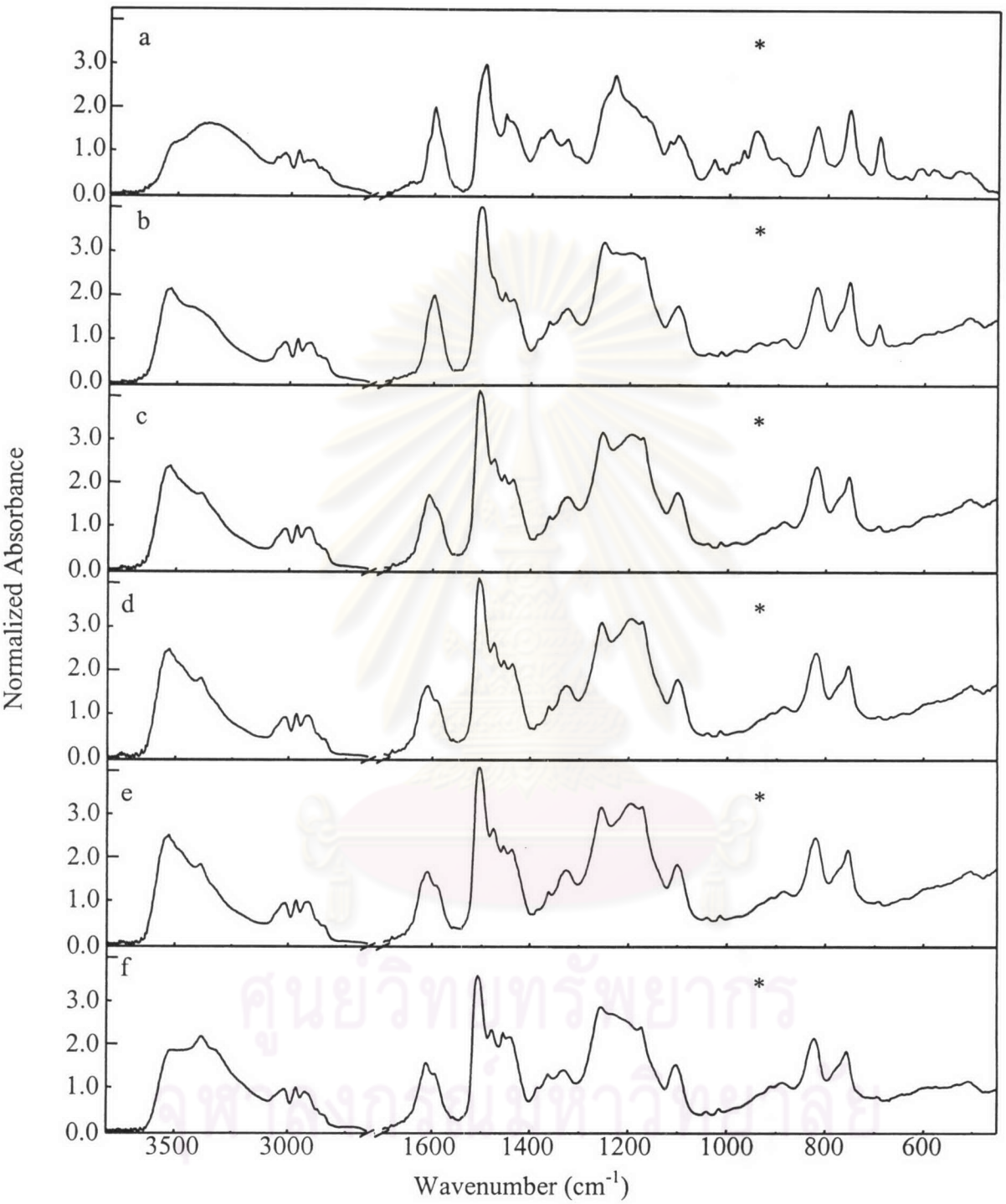


**Figure 4.24** FT-IR curing spectra of BP12. (a) before heating, (b) 200 °C, (c) 200 °C for 5 min, (d) 200 °C for 60 min, (e) 200 °C for 120 min, and (f) after cooling down to room temperature.

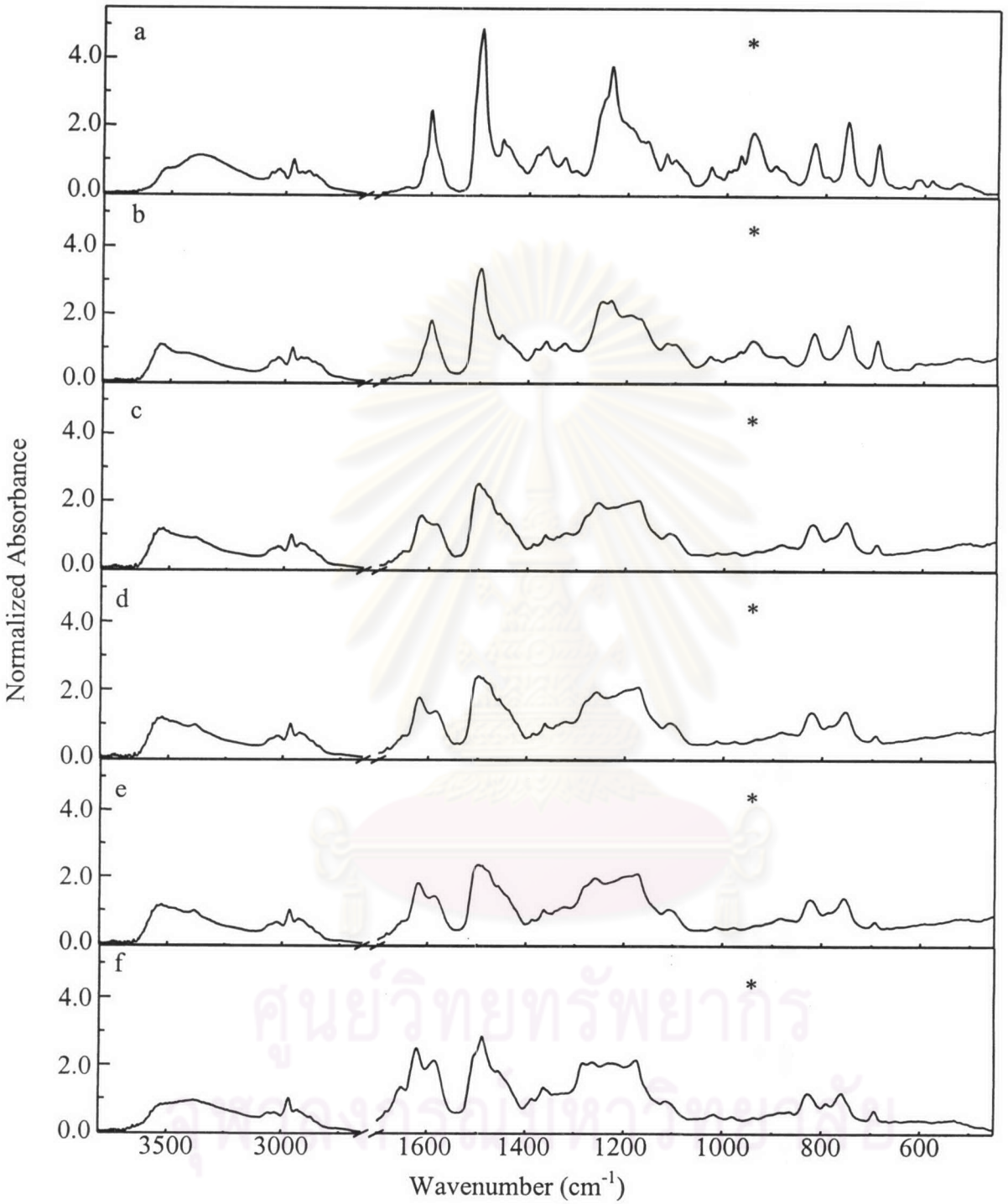


**Figure 4.25** FT-IR curing spectra of BP21. (a) before heating, (b) 200 °C, (c) 200 °C for 10 min, (d) 200 °C for 60 min, (e) 200 °C for 120 min, and (f) after cooling down to room temperature.

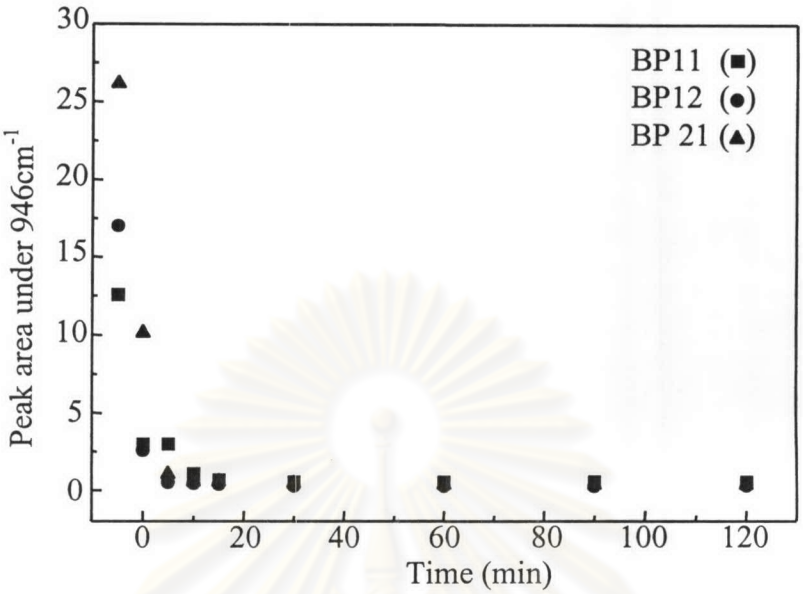


**Figure 4.26** Extent of the reaction observed at 946 $cm^{-1}$.

According to the observed phenomena, it can be concluded that the polymerization of benzoxazine with phenolic novolac takes place first. Then, as temperature increasing, the copolymerization of benzoxazine and epoxy proceeds quicker than the polybenzoxazine homopolymerization.

Figure 4.27 shows the DSC thermograms of the binary mixtures of epoxy and phenolic novolac resins. The thermograms show no exotherm maxima within the observed temperature range. However, the onsets of exothermic peaks are observed. This indicates that the reaction between these two resins slightly occurred within the observed temperature range. Figures 4.28 and 4.29 show the FT-IR curing spectra of EP11 at 100 °C and 200 °C, respectively. In both cases, the absorption band at 913 $cm^{-1}$ disappeared. It means that the reaction between epoxy and phenolic novolac resins occur. This is also confirmed by the appearance of new bands at 1335 $cm^{-1}$, assigned to the C-O(-Ar) symmetric stretching of aliphatic aromatic ether linkage.

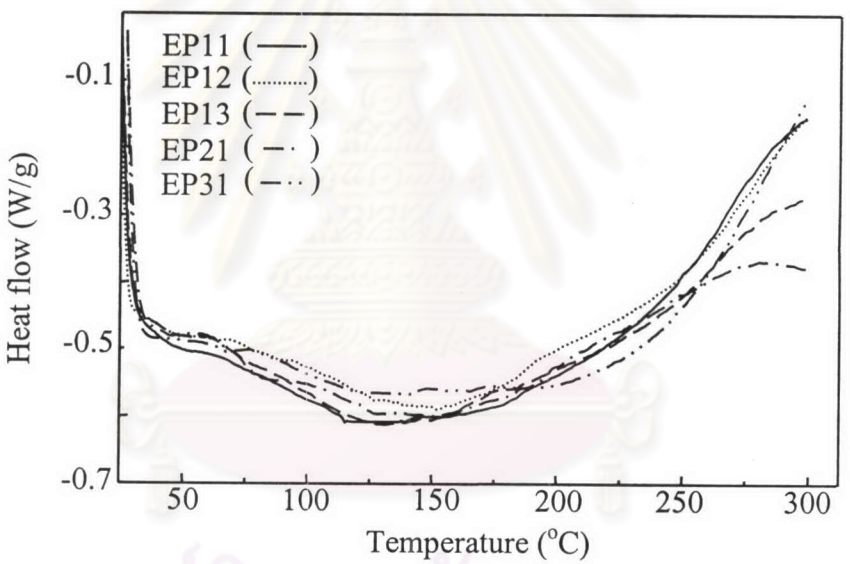


**Figure 4.27** DSC thermograms of the binary mixtures of epoxy and phenolic novolac resins.

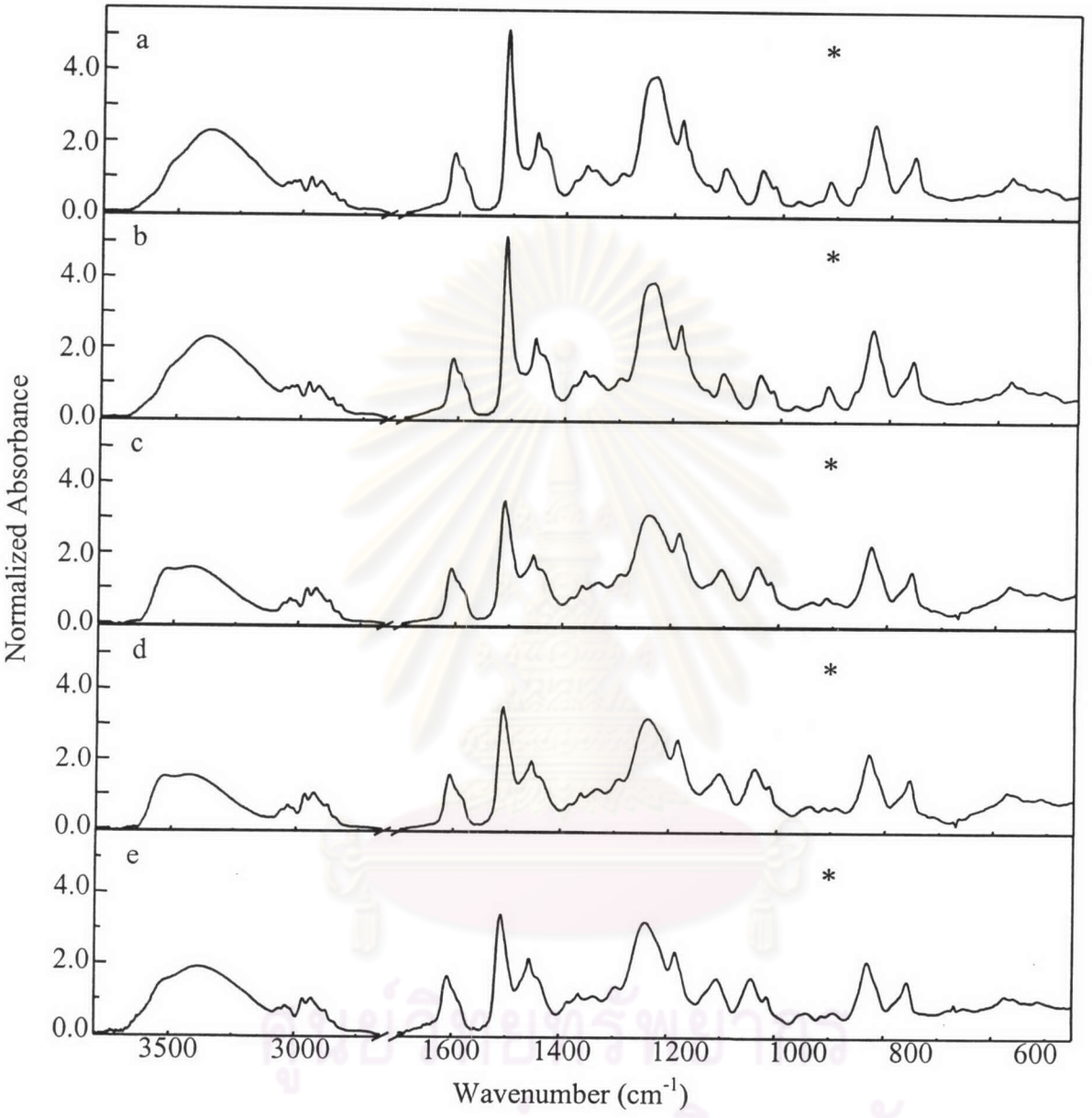


**Figure 4.28** FT-IR curing spectra of EP11. (a) before heating, (b) 100 °C, (c) 100 °C for 60 min, (d) 100 °C for 120 min, and (e) after cooling down to room temperature.

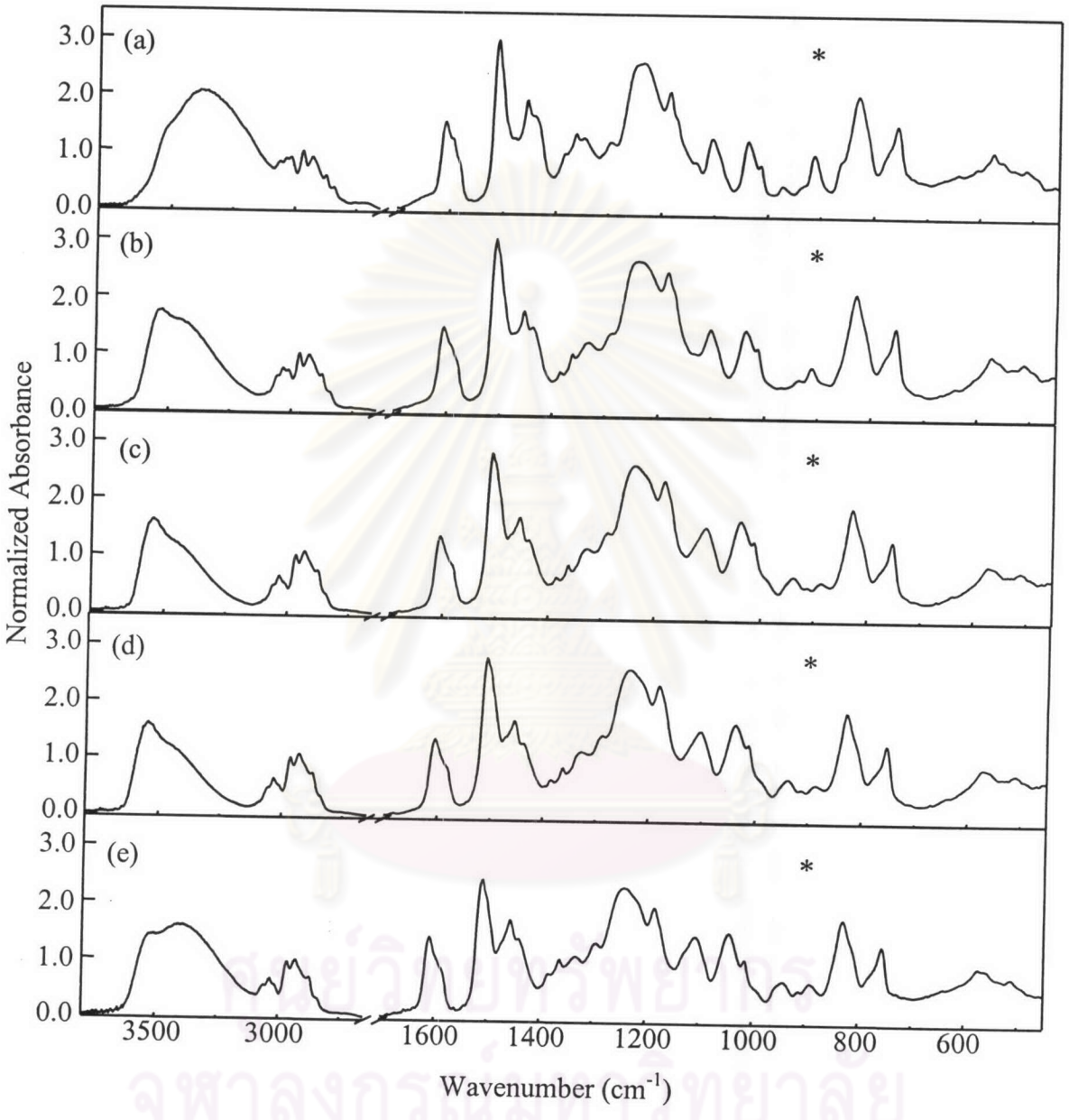


**Figure 4.29** FT-IR curing spectra of EP11. (a) before heating, (b) 200 °C, (c) 200 °C for 60 min, (d) 200 °C for 120 min, and (e) after cooling down to room temperature.

## 4.4 Reaction Kinetics of Ternary Systems

Form figures 4.2 and 4.3, when the amount of phenolic novolac resin is fixed at 20% by weight and the amounts of benzoxazine and epoxy resins are varied, the ternary mixtures show higher thermal stability. Figure 4.30 shows the DSC thermograms of these ternary mixtures. In all cases, single exothermic peaks are observed. The exothermic peaks of ternary mixtures shift to lower temperature with increasing amount of benzoxazine resin in the system. Figures 4.31 - 4.36 show the temperature dependent FT-IR spectra of these ternary mixtures. Figure 4.37 presents the extent of reaction at 946 $cm^{-1}$.

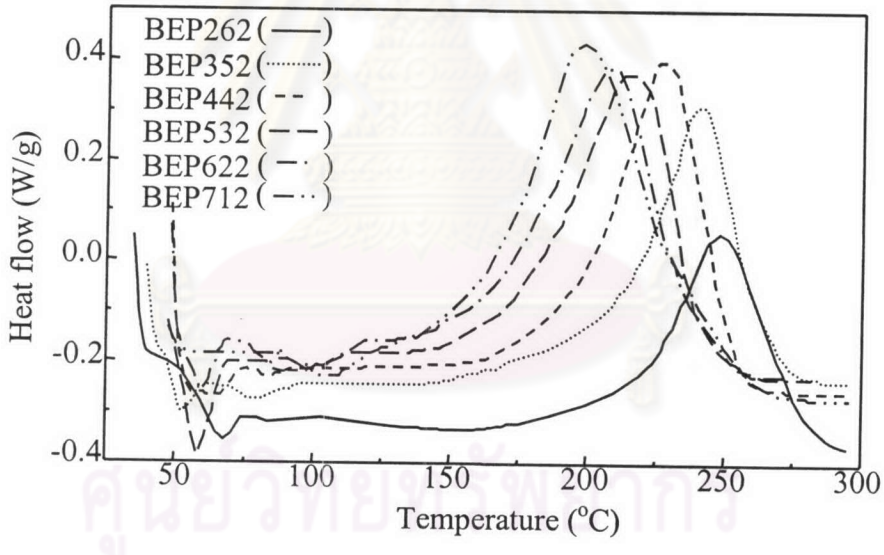


**Figure 4.30** DSC thermograms of ternary mixtures of benzoxazine, epoxy, and phenolic novolac resins.

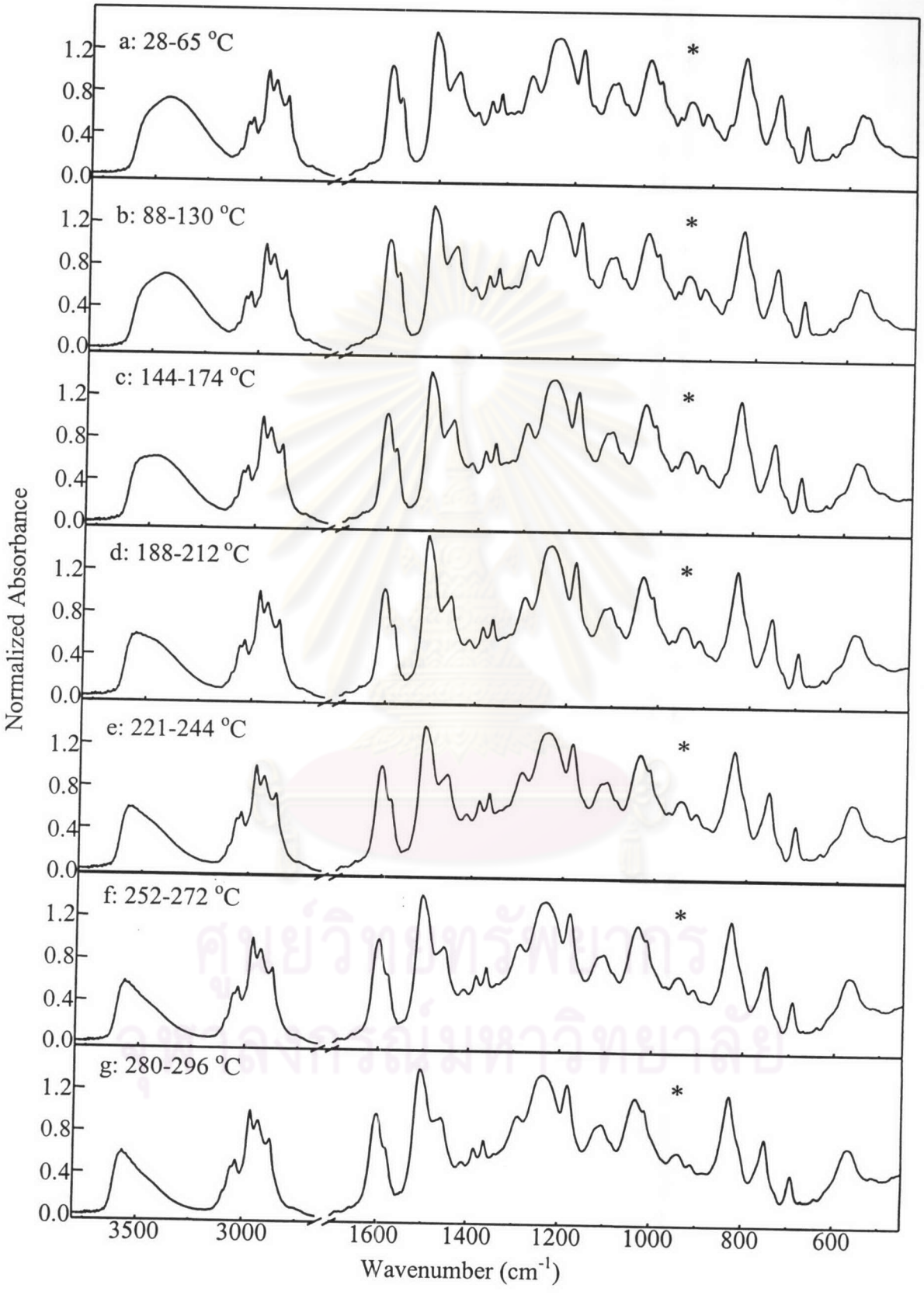


**Figure 4.31** FT-IR spectra of BEP262.

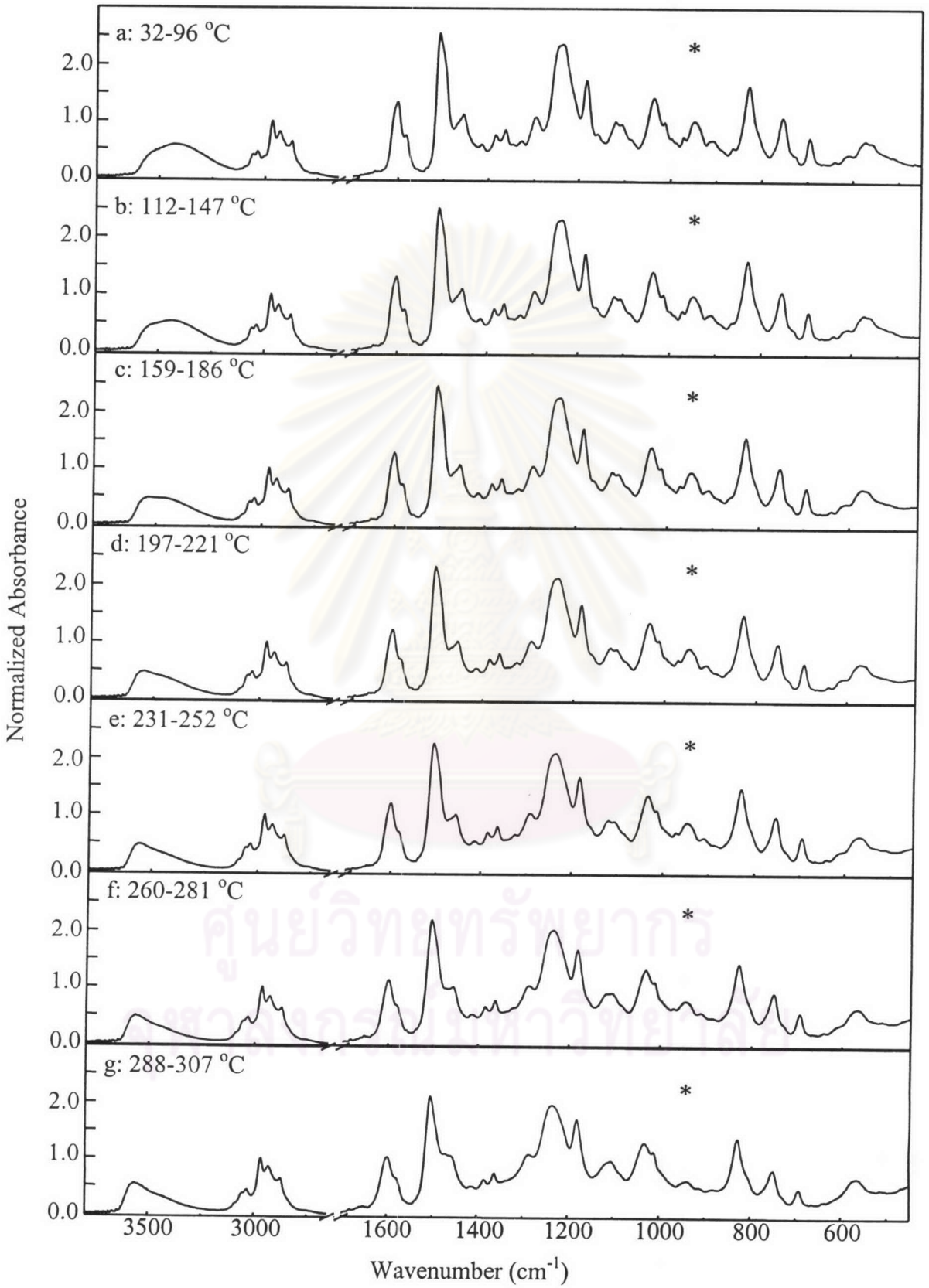


**Figure 4.32** FT-IR spectra of BEP352.

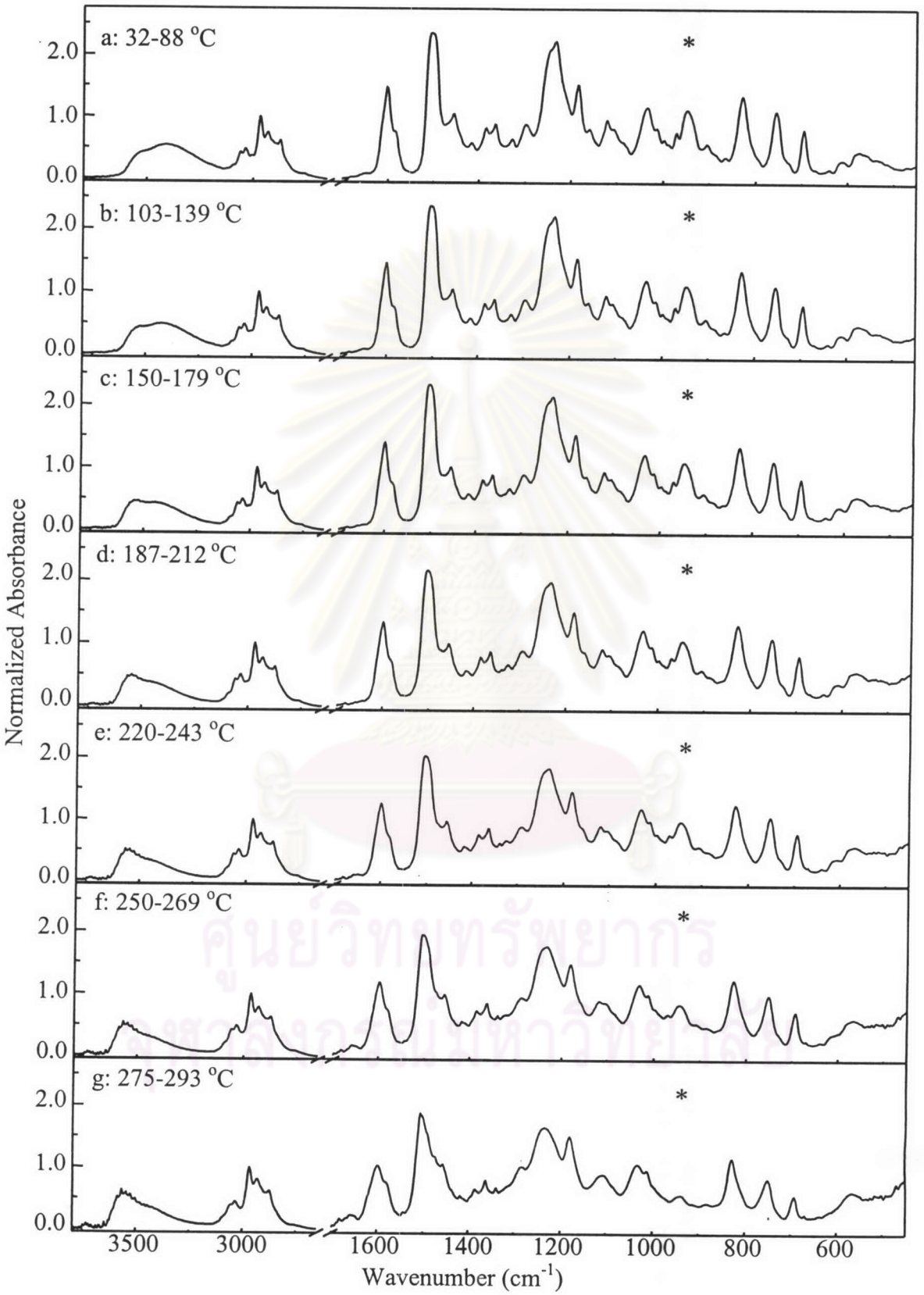


**Figure 4.33** FT-IR spectra of BEP442.

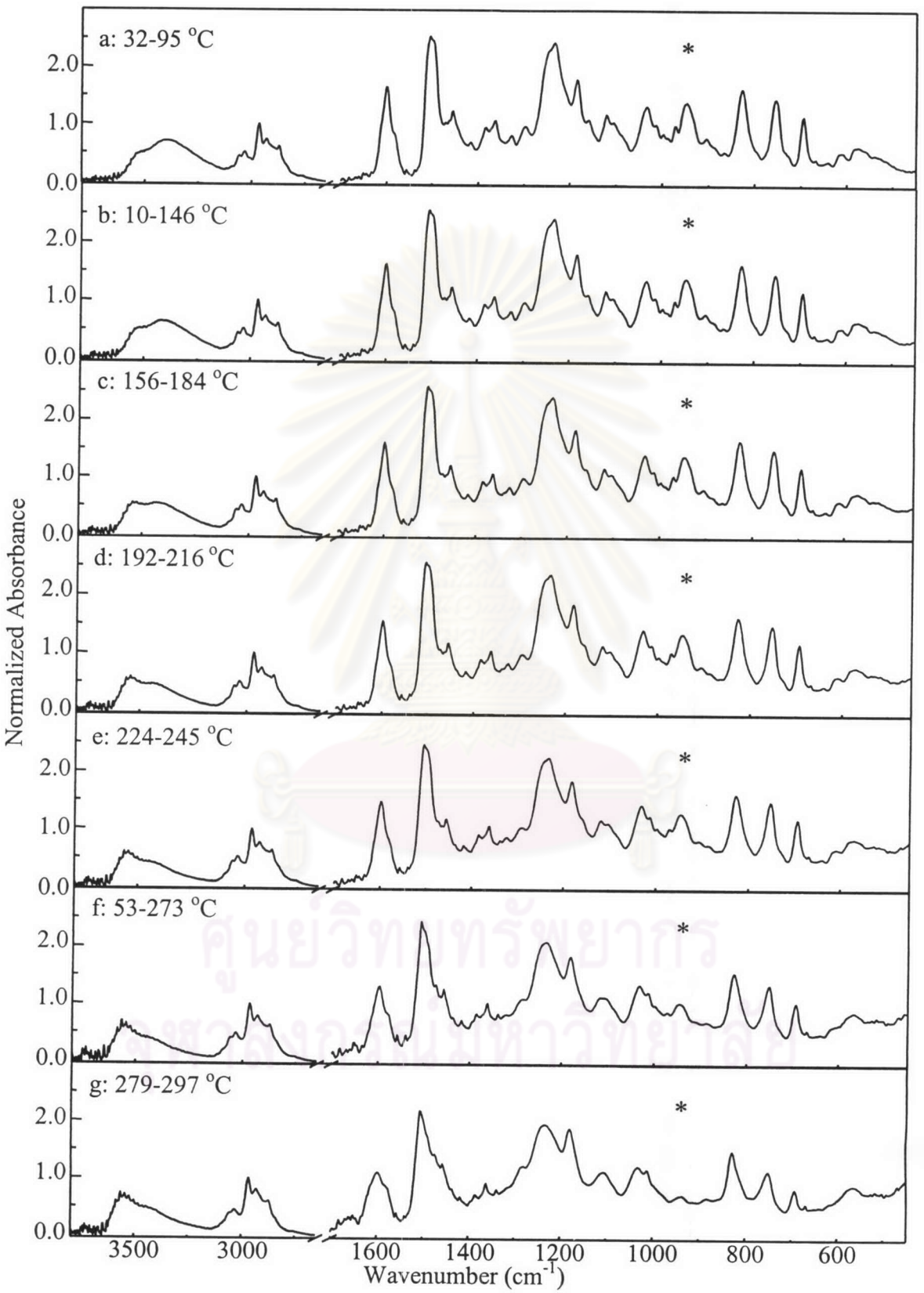


**Figure 4.34** FT-IR spectra of BEP532.

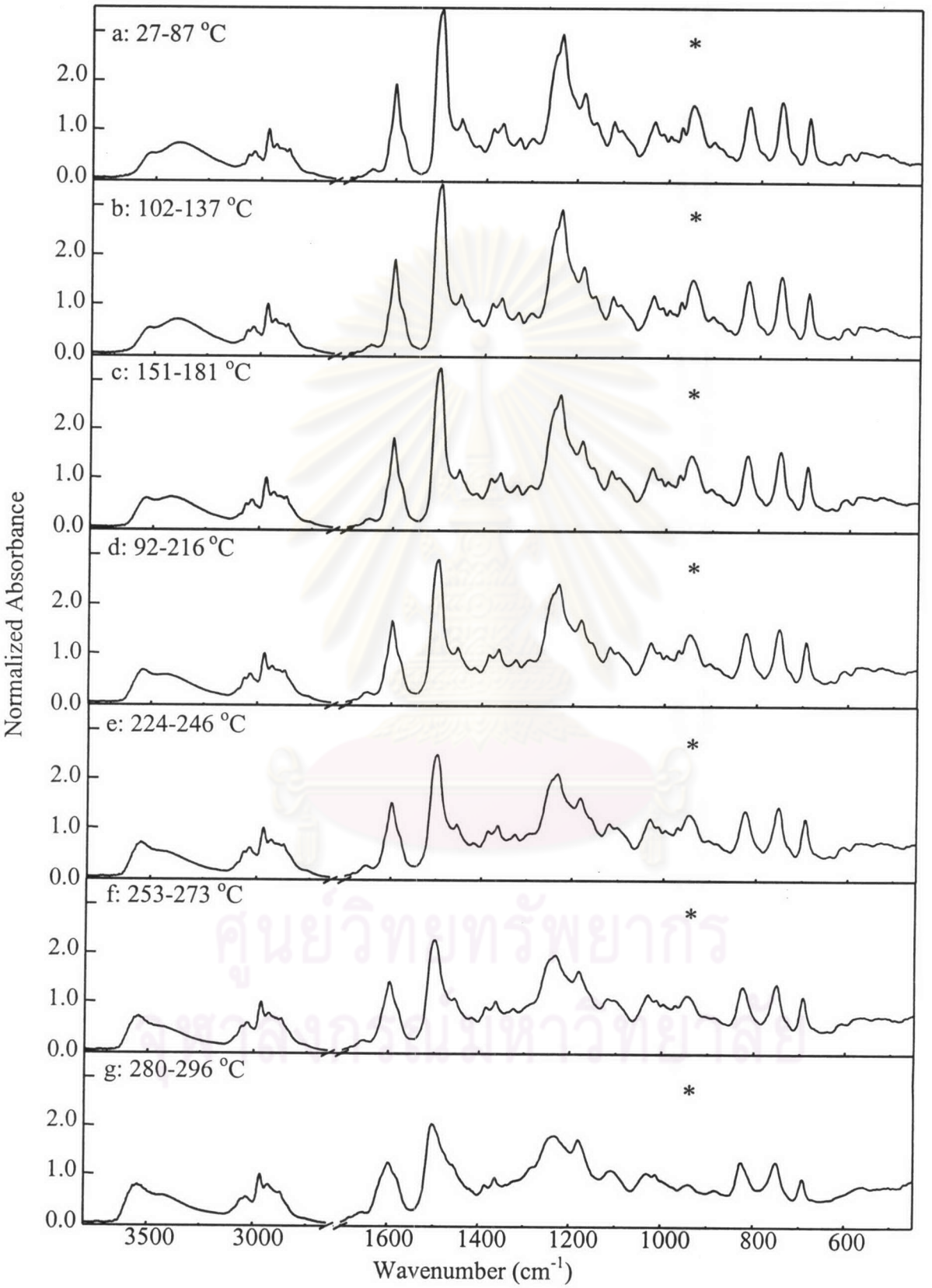


**Figure 4.35** FT-IR spectra of BEP622.

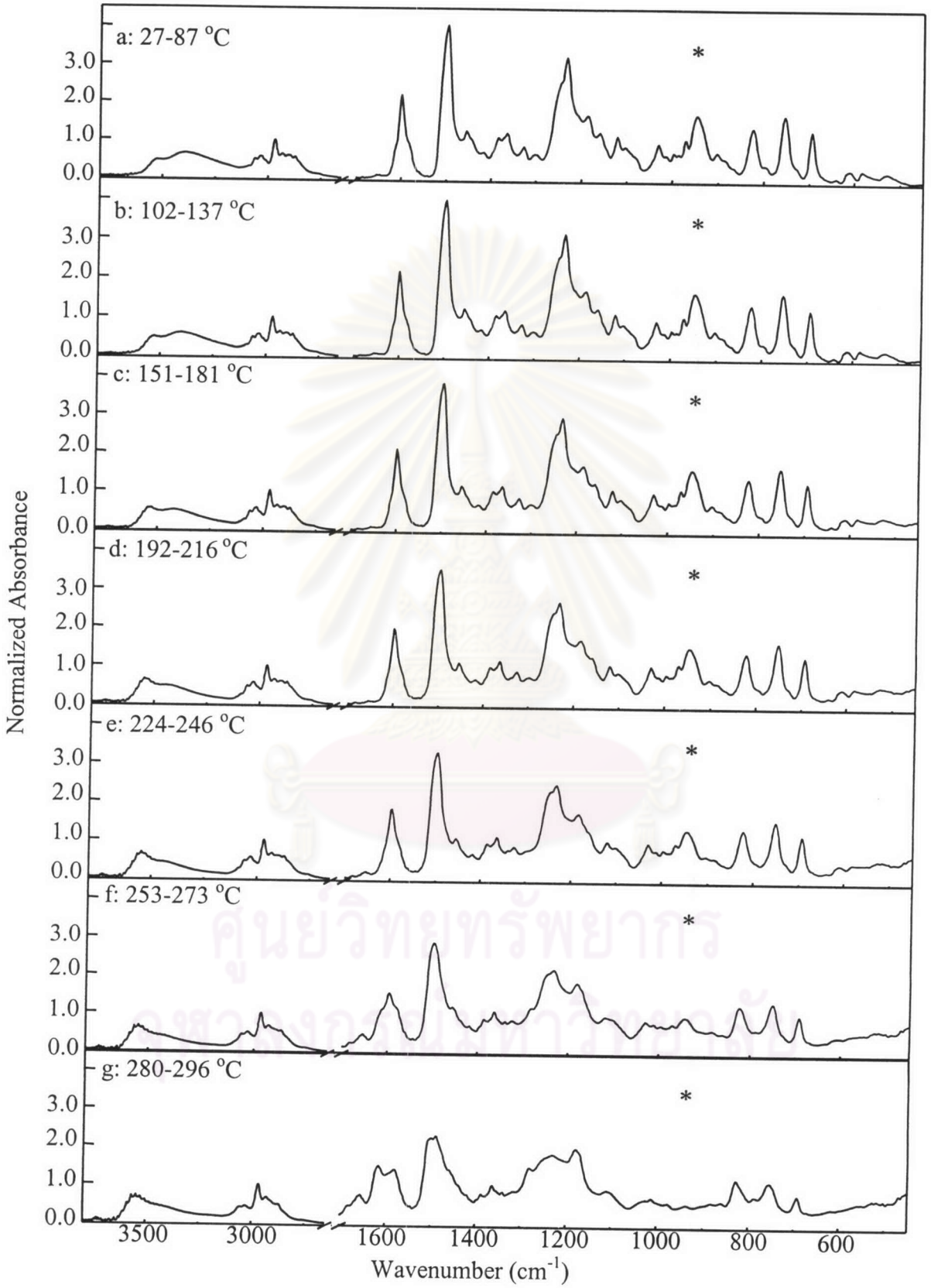


**Figure 4.36** FT-IR spectra of BEP712.

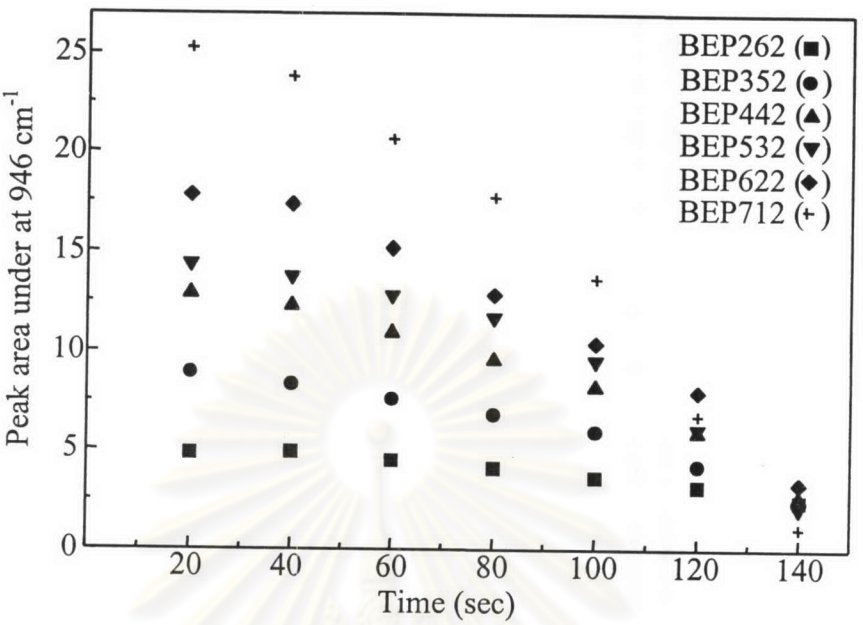


**Figure 4.37** Extent of the reaction at 946 $cm^{-1}$.

As mentioned before, BEP352 is chosen for further analysis. Non-isothermal DSC experiments at various heating rates is performed and their results are shown in figure 4.38. A single peak is observed in all DSC curves, which is similar to that of polybenzoxazine homopolymer. However as an overall process, changes may occur by two or more simultaneous or very close chemical reaction.

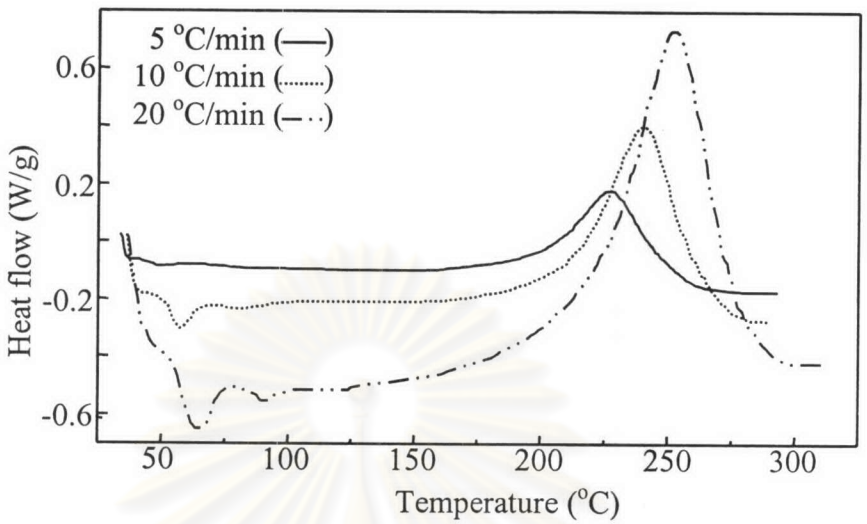


**Figure 4.38** DSC thermograms of BEP352.

It is assumed that there is no volatile compound released in sample pans that can affect the reaction kinetics. Thus, it can relate the area under the exotherm to the heat of reaction. Table 4.2 shows the total heat of reaction calculated at various heating rates. At slow heating rates some of the reaction occurred at the beginning. However, the end of the reaction is not recorded due to the lack of calorimeter sensivity. At the faster heating rates, degradation or other kinds of secondary reactions could also interfere in the determination of $\Delta H_R$. As a result, the total heat of reaction is averaged from those heating rates and was determined to be 155 J/g.

**Table 4.2** Total heat of reaction calculated at various heating rates.

| Heating rate (°C/min) | Exothermic peak (°C) | Onset exotherm (°C) | $\Delta H_R$ (J/g) |
|---|---|---|---|
| 5 | 227 | 197 | 152 |
| 10 | 240 | 210 | 155 |
| 20 | 252 | 218 | 158 |

To evaluate the kinetic parameter, a basic kinetic analysis was performed. The activation energy is calculated by Kissinger's and Ozawa's methods. The plots suggested by Kissinger's and Ozawa's methods are shown in figures 4.39 and 4.40, respectively.

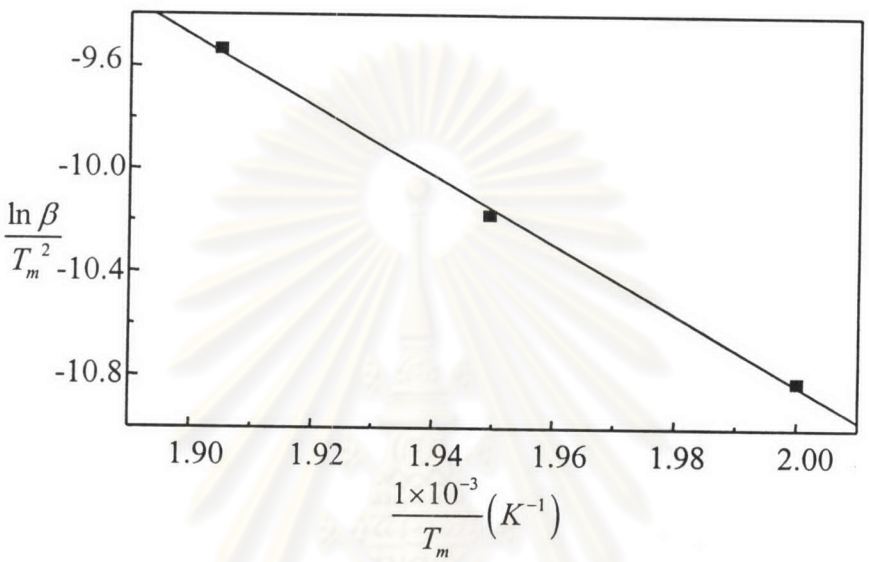


**Figure 4.39** Kissinger's plot for activation energy determination of BEP352.

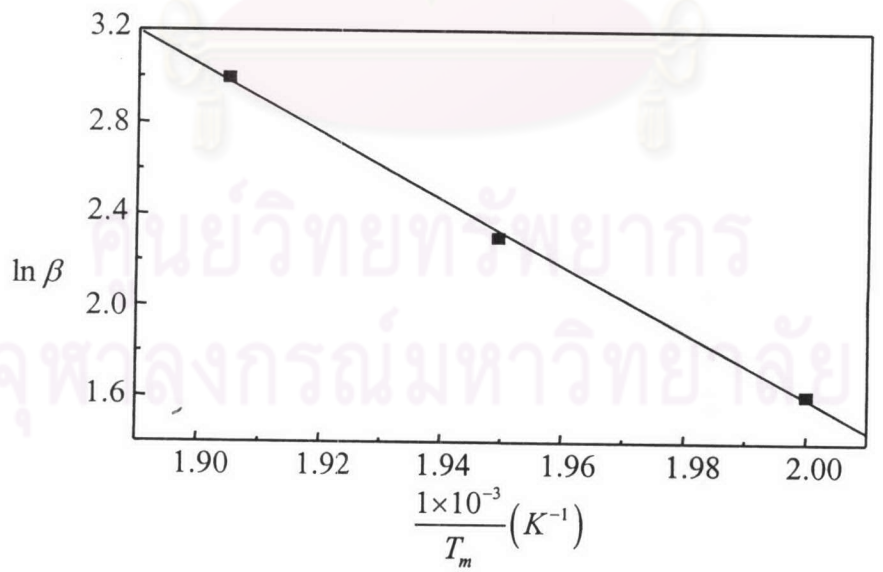


**Figure 4.40** Ozawa's plot for activation energy determination of BEP352.

The calculated values of $E_a$ are 112.35 and 120.86 kJ/mol by Kissinger's and Ozawa's methods, respectively.

To evaluate the reaction order, the mechanistic model is assumed. It is assumed that curing reaction of the ternary mixtures follow an $n^{th}$ order mechanism. The assumption would then be tested against the experimental data. Equation 2.5 can be re-written in logarithm form:

$$\ln\left(\frac{d\alpha}{dt}\right) = \ln Af(\alpha) - \frac{E_a}{RT} \tag{4.1}$$

Thus a plot of $\ln\left(\frac{d\alpha}{dt}\right)$ against $T^{-1}$ should provide a straight line with a slope equal $-\frac{E_a}{RT}$ and an intercept of $Af(\alpha)$.

The plots of $\ln\left(\frac{d\alpha}{dt}\right)$ against $T^{-1}$ for activation energy determination of BEP352 at various heating rates are shown in figures 4.41 - 4.43.

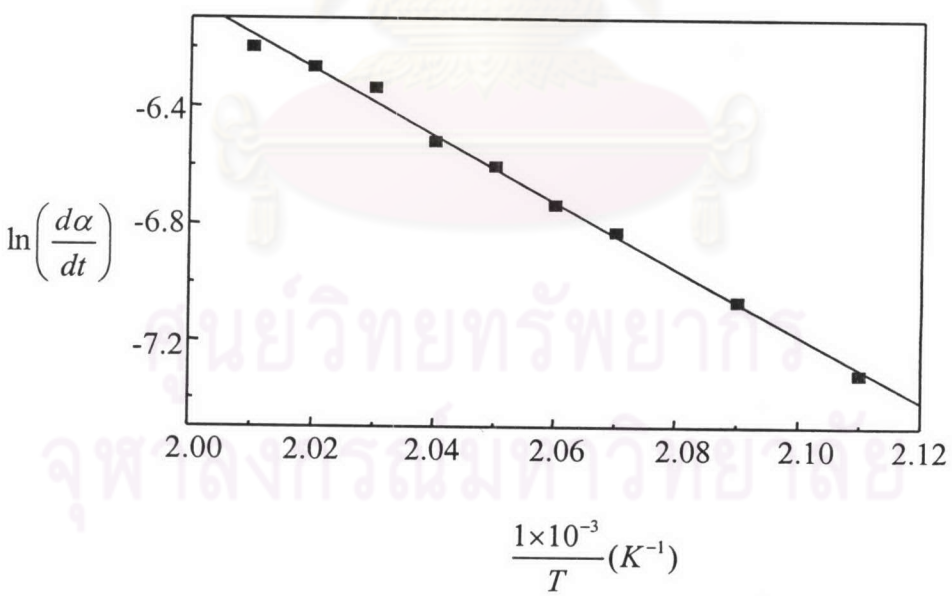


**Figure 4.41** Plot of $\ln\left(\frac{d\alpha}{dt}\right)$ and $\frac{1}{T}$ of BEP352 at 5 °C/min.

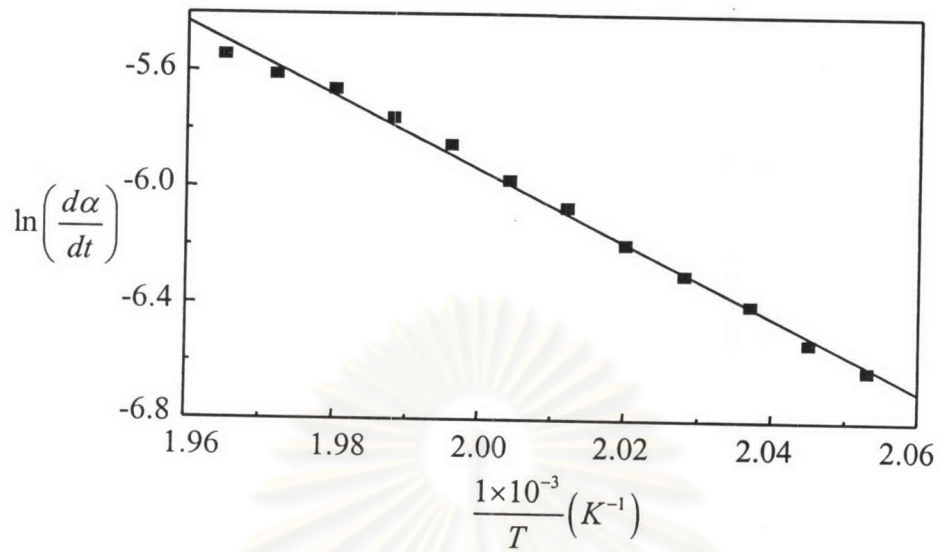


**Figure 4.42** Plot of $\ln\left(\frac{d\alpha}{dt}\right)$ and $\frac{1}{T}$ of BEP352 at 10 °C/min.

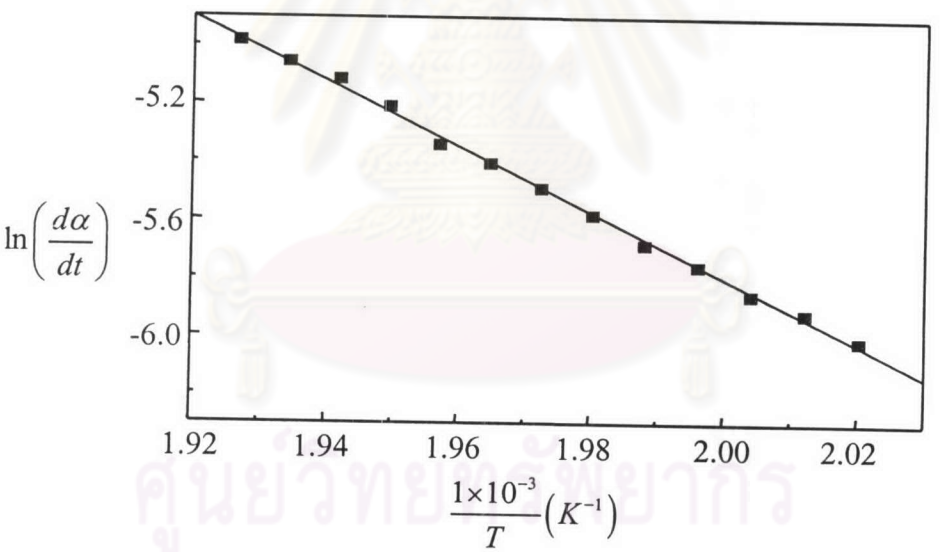


**Figure 4.43** Plot of $\ln\left(\frac{d\alpha}{dt}\right)$ and $\frac{1}{T}$ of BEP352 at 20 °C/min.

The mathematics of this model is expressed in equation 2.11. By substituting the Arrhenius equation for $k$ into equation 2.11 and take logarithmic of the result, the following expression is obtained:[3]

$$\ln\left(\frac{d\alpha}{dt}\right) = \ln A - \frac{E_a}{RT} + n\ln\left(1-\alpha\right) \qquad (4.2)$$

So that a graph of $\ln\left(\frac{d\alpha}{dt}\right)$ against $\ln(1-\alpha)$ should be a straight line of slope *n*.

To check the validity of the kinetic model in equation 4.2, the plots of $\ln\left(\frac{d\alpha}{dt}\right)$ against $\ln(1-\alpha)$ were performed at various heating rates as shown in figures 4.44 - 4.46.

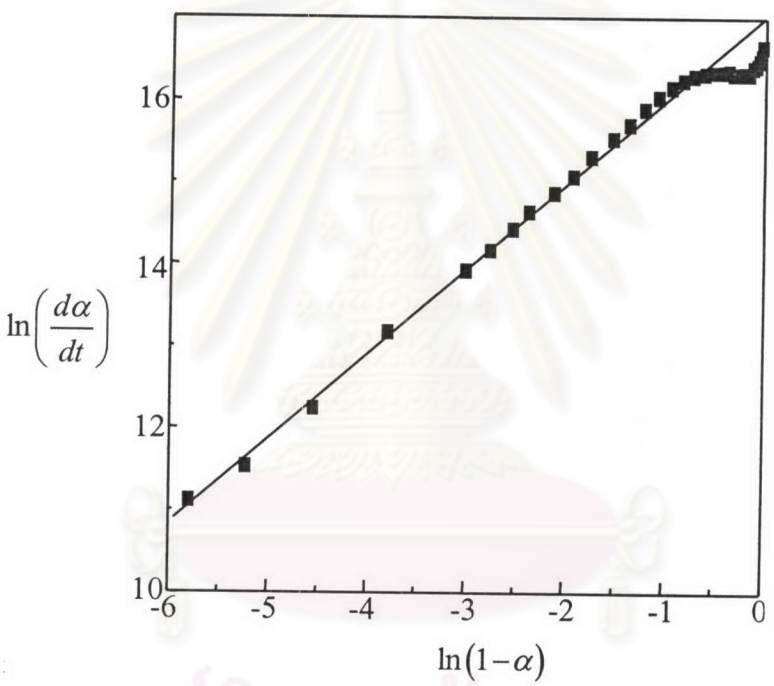


**Figure 4.44** Plot of $\ln\left(\frac{d\alpha}{dt}\right)$ and $\ln(1-\alpha)$ of BEP352 at 5 °C/min.

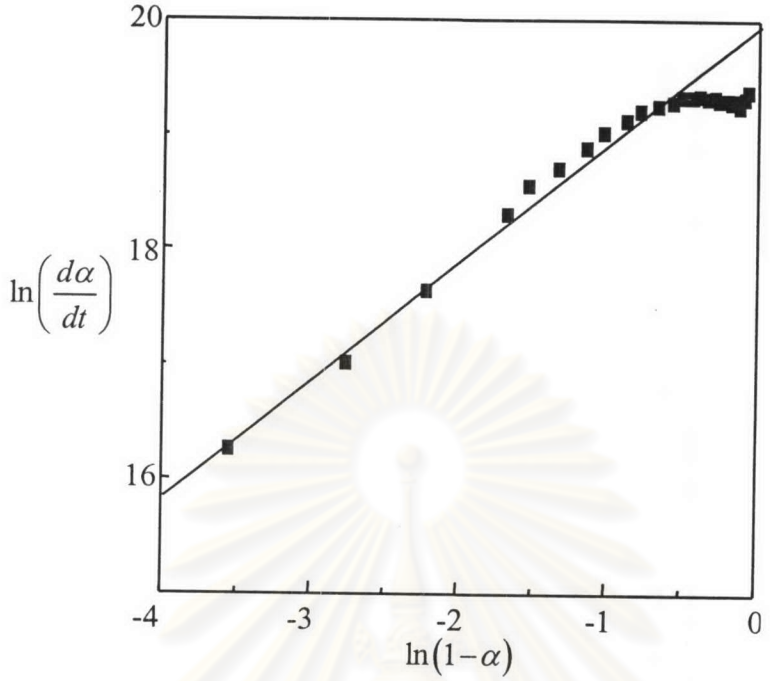


**Figure 4.45** Plot of $\ln\left(\frac{d\alpha}{dt}\right)$ and $\ln(1-\alpha)$ of BEP352 at 10 °C/min.

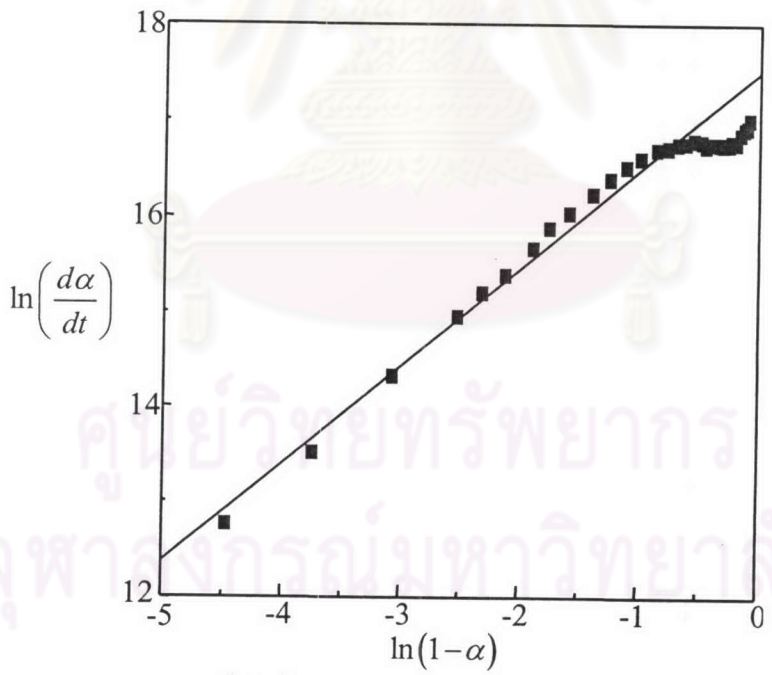


**Figure 4.46** Plot of $\ln\left(\frac{d\alpha}{dt}\right)$ and $\ln(1-\alpha)$ of BEP352 at 20 °C/min.

In all cases, the plots show the linear fit to the equation 4.2. Table 4.3 shows the differences between the activation energy and the reaction order calculated at various heating rates.

**Table 4.3** Activation energy and reaction order calculated at various heating rates.

| Heating rate (°C/min) | Activation energy (kJ/mol) | Reaction order |
|---|---|---|
| 5 | 92.96 | 1.03 |
| 10 | 104.93 | 1.03 |
| 20 | 93.78 | 1.02 |

Thus, it can be concluded that the curing reaction of BEP352 is the $n^{th}$ order kinetic. The activation energy is between 92.96 and 104.93 kJ/mol with the overall reaction order of approximately 1.03.

Figure 4.47 shows the FT-IR curing spectra of BEP352. Both the absorption 913 and 946 $cm^{-1}$ started to disappear within 100 °C for 120 minutes. It is due to the existence of phenolic novolac resin in the mixture. As a result, the reactions occur at the lower temperature than polybenzoxazine homopolymer, this is in good agreement with the previous reported. When the curing condition was at 100 °C for 120 minutes and then 120 °C for 120 minutes, the absorption at 913 $cm^{-1}$ disappeared (figure 4.47 (b)), while the absorption at 946 $cm^{-1}$ still remained. However this absorption band disappeared when the curing condition was at 100 °C for 120 minutes, 120 °C for 120 minutes, 150 °C for 120 minutes, 180 °C for 120 minutes, and then 200 °C for 90 minutes (figure 4.47 (f)). Thus it shows that the reaction between benzoxazine with phenolic novolac resins occurs first. Next, the copolymerization of benzoxazine and epoxy resin takes place, and then the polybenzoxazine homopolymerization occurs, respectively.

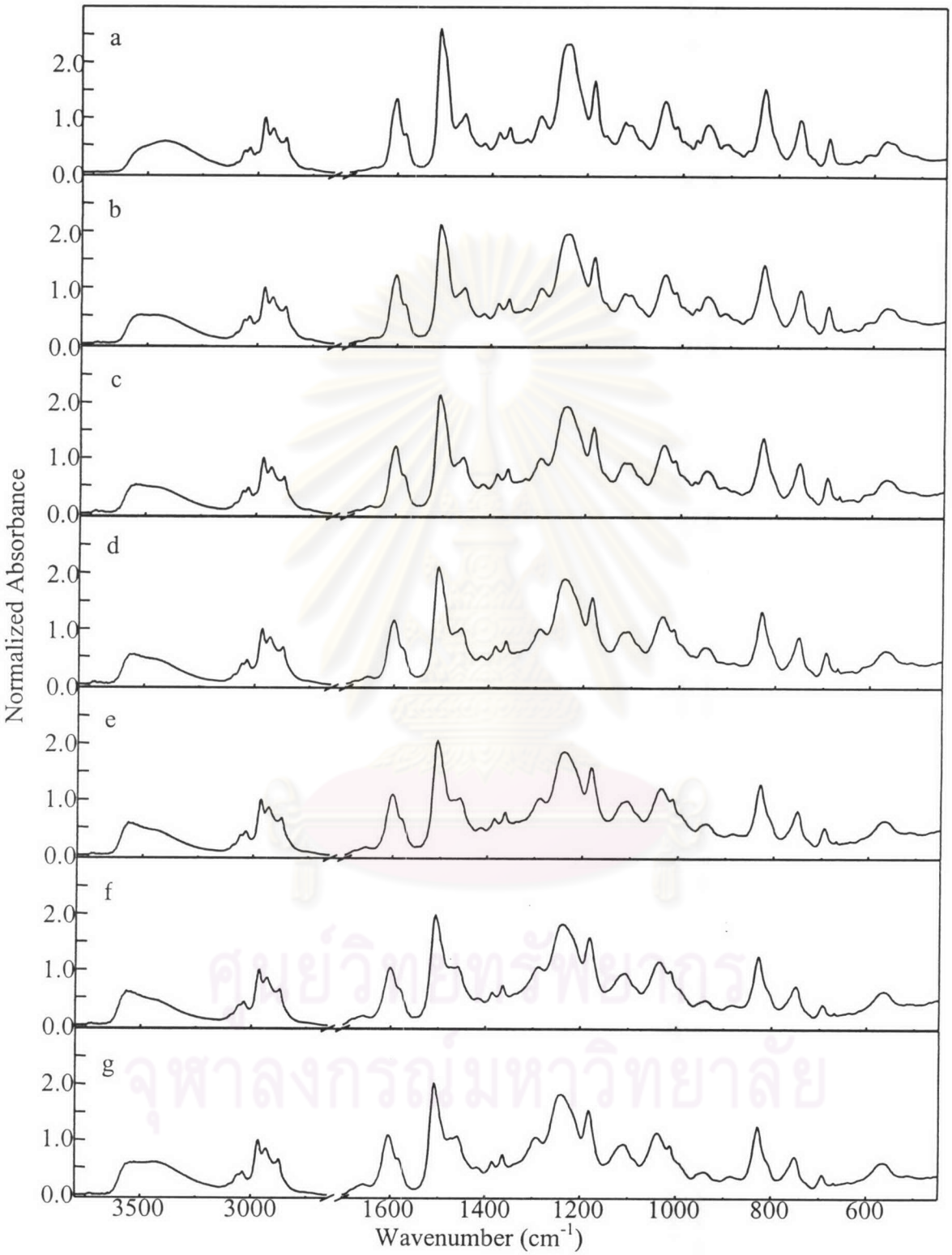


**Figure 4.47** FT-IR spectra of BEP352. (a) before reaction, (b) 100 °C/120 min, (c): (b) with 120 °C/120 min, (d): (c) with 150 °C/120 min, (e): (d) with 180 °C/120min, (f): (e) with 200 °C/90 min, and (g) after heating.

Figure 4.48 exhibits the FT-IR curing spectra of BEP352 at 200 °C. It is well known that the gelation time of benzoxazine was short.[39] This is because the benzoxazine ring opened and the phenolic hydroxyl groups that contributed to the curing reaction were produced easily. Figure 4.49 presents extent of the reaction at 946 $cm^{-1}$ as a function of curing time. Almost 100% of oxazine ring opened within 30 minutes. Since the gelation imposes mobility restrictions upon the chain, the kinetics will be affected. Therefore, the analysis of kinetic parameters will be calculated from the data up obtained up to 30 minutes.

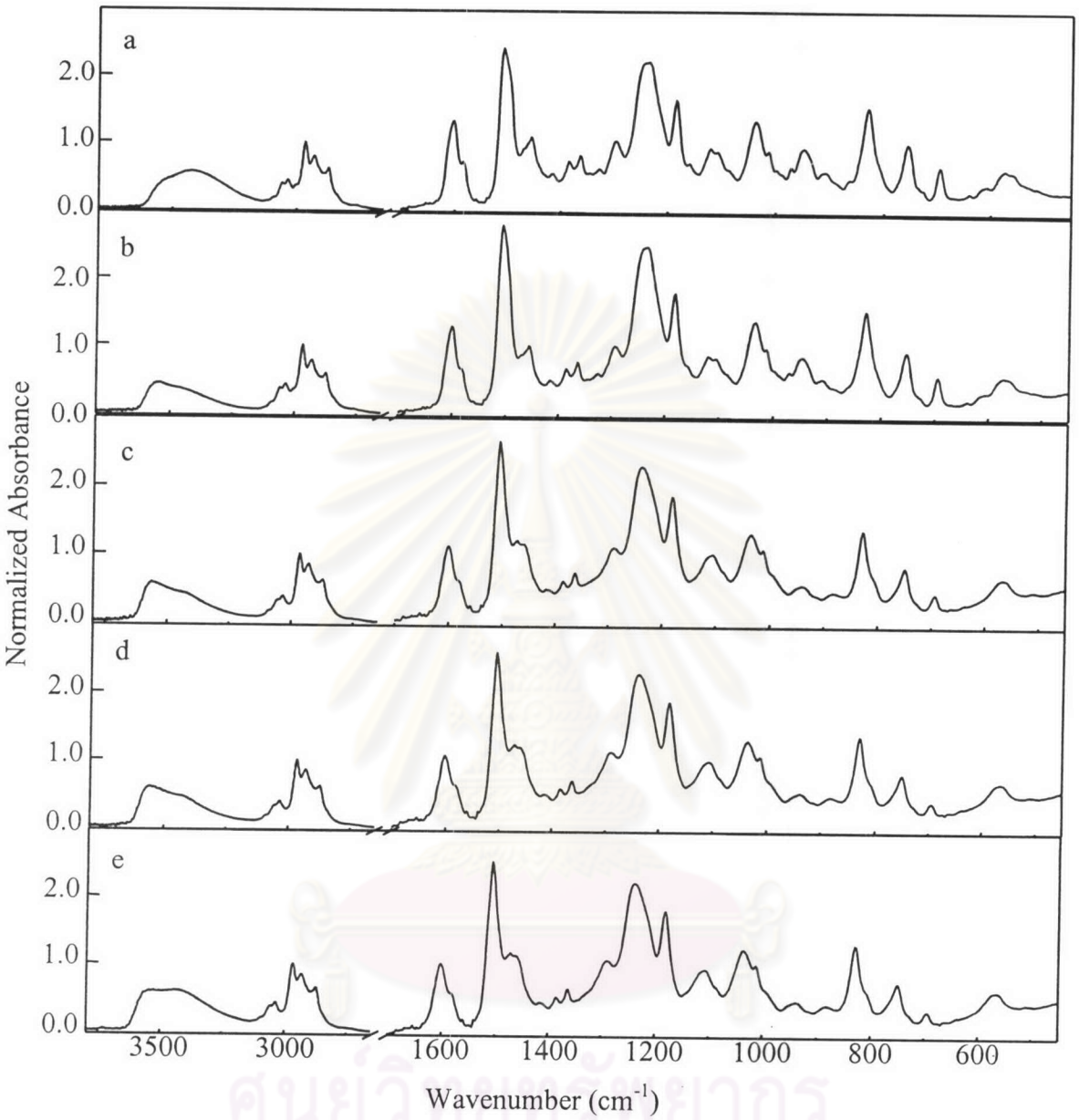


**Figure 4.48** FT-IR spectra of BEP352. (a) before heating, (b) 200 °C, (c) 200 °C for 60 min, (d) 200 °C for 120 min, and (e) after heating.

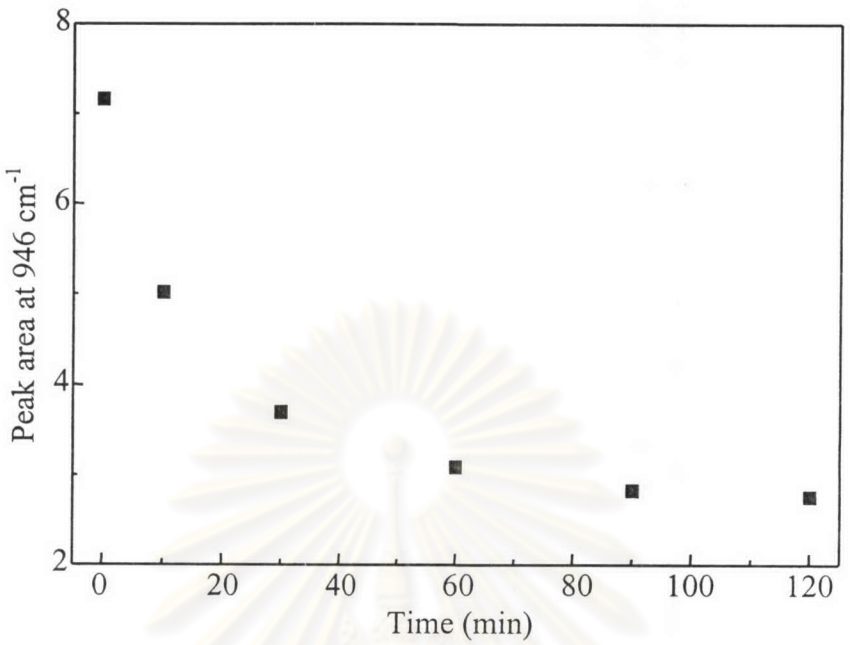


**Figure 4.49** Extent of the reaction at 946 $cm^{-1}$ of BEP352.

According to the Beer-Lambert's law, the absorbance observed in IR technique is linearly proportional to the concentration of sample. Due to the nonlinear heating rate in the hot cell, the reaction kinetics are calculated as a function of time rather than temperature. Thus the rate of change sample concentration can be expressed in general term as:[40]

$$-\frac{d[A]}{dt} = k[A]^n = kt \qquad (4.3)$$

where $\frac{d[A]}{dt}$ is the change of absorbance as a function of time, $k$ is the rate constant, and $n$ is the reaction order.

To determine the order of reaction, there are three ways of plotting the absorbance as a function of time: [40]

(i) the zero order reaction (i.e., $n = 0$)

$$A(\lambda)_0 - A(\lambda) = -kt \tag{4.4}$$

(ii) the first order reaction (i.e., $n = 1$)

$$\ln\left[\frac{A(\lambda)_0}{A(\lambda)}\right] = -kt \tag{4.5}$$

and (iii) the second order reaction (i.e., $n = 2$)

$$\frac{1}{A(\lambda)} - \frac{1}{A(\lambda)_0} = kt \tag{4.6}$$

Only the second case gave a straight line. Therefore, reaction is the first order. The rate constant $k$ can be derived from the slope of the line ($k = 0.1095$ sec$^{-1}$), as shown in figure 4.50.

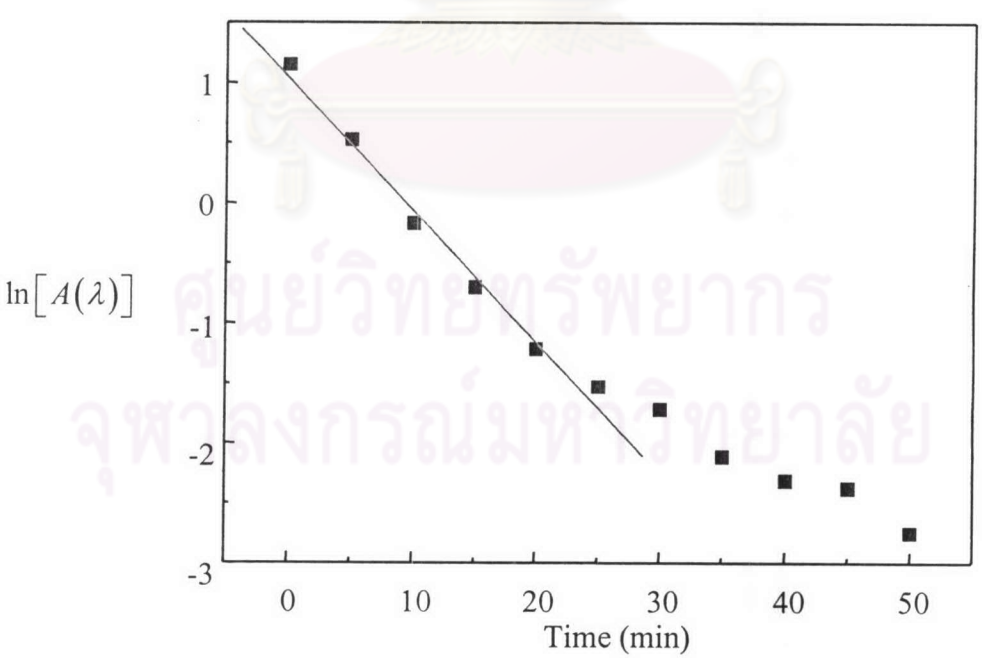


**Figure 4.50** Plot of $\ln[A(\lambda)]$ and time of BEP352 at 946 cm$^{-1}$.